

# Barriers to Internal Rotation in Neopentylbenzenes Substituted on the Benzyl Group. A $^{13}\text{C}$ NMR Band Shape Study

Sven Andersson\* and Torbjörn Drakenberg†

Organic Chemistry 2, Chemical Centre, University of Lund, S-220 07 Lund, Sweden

Two series of neopentylbenzenes with one or two substituents on the benzyl group have been synthesized. In one series the substituents were H, F, Cl, Br, I, OCH<sub>3</sub>, OCOCH<sub>3</sub>, OSi(CH<sub>3</sub>)<sub>3</sub>, CH<sub>3</sub> and CH<sub>2</sub>CH<sub>3</sub>, and in the other OH and R [R = H, CH<sub>3</sub>, CH<sub>2</sub>CH<sub>3</sub>, (CH<sub>2</sub>)<sub>3</sub>CH<sub>3</sub>, CH(CH<sub>3</sub>)<sub>2</sub> and C(CH<sub>3</sub>)<sub>3</sub>]. Barriers to internal C<sub>sp<sup>3</sup></sub>-C<sub>sp<sup>2</sup>(aryl)</sub> and C<sub>sp<sup>3</sup></sub>-C<sub>sp<sup>3</sup></sub> rotation have been estimated by  $^{13}\text{C}$  NMR band shape methods. Estimated barriers were found to increase as the size of the substituent increases. The results are discussed in terms of possible initial and transition states, based on summations of results from molecular mechanics (MM) calculations, using the Allinger MMP1 program. Barriers estimated experimentally are compared with results from other systems found in the literature.

## INTRODUCTION

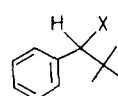
In our studies of substituent effects in the 1,3,5-trineopentylbenzene (TNB) system, we wished to include TNB compounds with substituents on the benzyl group, since most TNB compounds previously studied have been substituted in the aromatic ring.<sup>1a-b</sup> Baas and Sinnema<sup>2</sup> studied two TNB compounds containing (H, OH) and (CH<sub>3</sub>, OH) groups as benzylic substituents by  $^1\text{H}$  NMR spectroscopy, and found that the low-temperature spectra were very complex owing to the presence of different rotamers. Our aim was first to study benzylically substituted mononeopentylbenzenes, because in this case complete band shape analysis can be employed. The mononeopentylbenzenes would then be used as model substances, since the barriers are expected to be similar in the two series.<sup>2</sup>

Reuvers *et al.*<sup>3a,b</sup> synthesized ring-substituted neopentylbenzenes and studied the internal C<sub>sp<sup>3</sup></sub>-C<sub>sp<sup>2</sup>(aryl)</sub> rotation by  $^1\text{H}$  NMR spectroscopy. The barriers (usually low) to internal rotation could be estimated in some cases. Neopentylbenzenes substituted in the benzylic position have been studied by  $^1\text{H}$  NMR spectroscopy. Baas *et al.*<sup>4a,4b</sup> studied the internal C<sub>sp<sup>3</sup></sub>-C<sub>sp<sup>2</sup>(aryl)</sub> rotation in 4-alkyl-2-nitroacetanilides and in  $\alpha$ -alkyl-substituted (3,4,5-trimethoxy)phenyl-*tert*-butylcarbinols. Gall *et al.*<sup>5a</sup> and Newsoroff and Sternhell<sup>5b</sup> studied the internal rotation in *tert*-butylphenyl- and di-*tert*-butylphenyl-carbinols, substituted in the 3-, 4- and 5-positions in the aromatic rings.

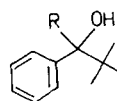
As an aid for our studies, the following neopentylbenzenes were synthesized, all of which were studied as racemates except, of course, the achiral compounds **1** and **16**.

\* Author to whom correspondence should be addressed.

† Physical Chemistry 2, Chemical Center, University of Lund, S-220 07, Lund, Sweden.



1	X = H	7	X = OCOCH <sub>3</sub>
2	F	8	OSi(CH <sub>3</sub> ) <sub>3</sub>
3	Cl	9	CH <sub>3</sub>
4	Br	10	CH <sub>2</sub> CH <sub>3</sub>
5	I		
6	OCH <sub>3</sub>		



11	R = H
12	CH <sub>3</sub>
13	CH <sub>2</sub> CH <sub>3</sub>
14	CH <sub>2</sub> (CH <sub>2</sub> ) <sub>2</sub> CH <sub>3</sub>
15	CH(CH <sub>3</sub> ) <sub>2</sub>
16	C(CH <sub>3</sub> ) <sub>3</sub>

## EXPERIMENTAL

### NMR measurements

The  $^{13}\text{C}$  NMR band shape method was used to study barriers to internal C<sub>sp<sup>3</sup></sub>-C<sub>sp<sup>2</sup>(aryl)</sub> and C<sub>sp<sup>3</sup></sub>-C<sub>sp<sup>3</sup></sub> rotation. In most cases, NMR spectra were recorded at at least 10 different temperatures. The rate constants were estimated from visual fitting of plotted to experimental spectra.

Wherever possible, the transverse relaxation time ( $T_2$ ) was determined at both the high and low temperature limits for the exchanging signal and for a reference signal ( $T_2^{\text{ref}}$ ) originating from a nucleus in the same molecule. At intermediate temperatures,  $T_2$  was interpolated by the use of Eqn (1).<sup>6a,b</sup>

$$T_2^{-1} = (T_2^{\text{ref}})^{-1} + \pi \Delta\nu_{\text{corr}} \quad (1)$$

$\Delta\nu_{\text{corr}}$  is a correction factor and is assumed to vary linearly with temperature. In cases where only high (low) temperature data on  $T_2$  and  $T_2^{\text{ref}}$  could be obtained, these values were extrapolated to low (high) temperatures.

Determination of chemical shifts at temperatures where this parameter could not be estimated by band fitting was carried out by extrapolation from data below the coalescence temperature.

$^{13}\text{C}$  NMR spectra used for band shape analysis were recorded on a Varian XL-100 spectrometer operating at 25 MHz in the Fourier transform mode. To obtain a spectrum *ca* 4000 pulses were used.

The temperature was measured by means of a copper-constantan thermocouple, which was fixed near the receiver coil. The accuracy in these values has been shown to be better than  $\pm 2^\circ\text{C}$  and is reproducible within  $\pm 0.5^\circ\text{C}$ .<sup>1b</sup>

Band shape analyses involving calculations of theoretical spectra for exchange between two sites were performed on an HP 9820 A calculator equipped with a plotter. The calculations of spectra for exchange between many sites were performed at the Lund University Computing Centre on a Univac 1100/80, equipped with a Calcomp plotter.

The first-order rate constants ( $k$ ), obtained from the band shape analyses, were used in conjunction with the Eyring equation<sup>7a</sup> to calculate the free energy of activation ( $\Delta G_T^\ddagger$ ) at each temperature ( $T$ ). The rate constants ( $k$ ) were defined as  $k = \tau_A^{-1}$ , where  $\tau_A$  is the lifetime at site A. The relative statistical errors in estimated  $\Delta G_T^\ddagger$  values were estimated by the approximate expression (2), which can be derived by analysis of the Eyring equation.<sup>7b</sup>

$$(\sigma \Delta G_T^\ddagger / \Delta G_T^\ddagger)^2 = [\ln 10(10.32 + \log Tk^{-1})]^{-2} (\sigma_k/k)^2 + (\sigma_T/T)^2 \quad (2)$$

where  $\sigma \Delta G_T^\ddagger$ ,  $\sigma_k$  and  $\sigma_T$  are the relative errors in  $\Delta G_T^\ddagger$ , rate constant and temperature, respectively.

For some compounds the enthalpy ( $\Delta H^\ddagger$ ) and entropy ( $\Delta S^\ddagger$ ) of activation were estimated from a plot of the estimated  $\Delta G_T^\ddagger$  versus  $T$ , as the intercept and the slope of the curve, respectively. The errors in  $\Delta H^\ddagger$  and  $\Delta S^\ddagger$  could be estimated from the plot of  $\Delta G_T^\ddagger$  versus  $T$  when the error bars in  $\Delta G_T^\ddagger$  were marked. The total uncertainty is thus represented by a rectangle. Two straight lines pivoting about the coalescence temperature and passing through the rectangle gave two different slopes and intercepts. The difference in these parameters was taken as the maximum error.<sup>8</sup>

## Calculations

The MMP1 program of Allinger *et al.*<sup>9a-2,10</sup> was used to calculate the energy for different conformations on the potential surface for internal  $\text{C}_{\text{sp}^3}\text{-C}_{\text{sp}^2(\text{aryl})}$  rotation in compounds **1**, **9**, **10** and in benzyl chloride. For compounds **9** and **10** the initial and transition states found were recalculated with a revised version of the Allinger program (MMP2).<sup>11,12</sup>

## RESULTS

For all compounds except **16** the ambient temperature ( $28^\circ\text{C}$ )  $^{13}\text{C}$  NMR spectra were of the type expected for rapidly rotating phenyl groups. For **16** the  $^{13}\text{C}$

NMR spectrum was more complex than those for the other compounds, and consequently a slowly rotating phenyl group was assumed.

The *tert*-butyl resonances in the  $^{13}\text{C}$  NMR spectra of all compounds appeared as a single line, indicating fast rotation at  $28^\circ\text{C}$ . The  $^{13}\text{C}$  NMR chemical shifts are summarized in Table 1.

The assignments of the unsubstituted aromatic carbons in Table 1 are based on the following assumptions: (a) at fast neopentyl rotation the *ortho* carbons are less shielded (owing to the substituent effect) and would then have a higher resonance frequency than the *meta* carbons;<sup>13a-c</sup> and (b) at slow neopentyl rotation a greater difference in chemical shift can be found between the two non-equivalent *ortho* carbons than between the two non-equivalent *meta* carbons.<sup>14</sup>

## Rotation around the $\text{C}_{\text{sp}^3}\text{-C}_{\text{sp}^2(\text{aryl})}$ bond

For compounds **1**, **2** and **11** the  $^{13}\text{C}$  NMR spectra of the aromatic carbons remained essentially the same down to the lowest temperatures attainable ( $-142^\circ\text{C}$  for **2** and  $-125^\circ\text{C}$  for **11**). For all other compounds, drastic changes occurred in the spectra as a function of temperature.

At temperatures where the neopentyl rotation is sufficiently slow, the aromatic carbons will reside in different chemical environments. The unsubstituted aromatic carbons are then expected to appear as five distinct peaks of equal intensities in the  $^{13}\text{C}$  NMR spectrum. This has been found for compounds **12**, **13** and **14** (see Fig. 1). The peaks were in all cases assigned as the two non-equivalent *ortho* carbons to low field, the two non-equivalent *meta* carbons and the *para* carbon peak to high field.

In the case of compounds **4**, **5**, **6**, **8** and **16** the same aromatic region showed only four resolvable peaks. For **4** and **6** these patterns were assigned as an overlap between one of the non-equivalent *meta* carbons and the *para* carbon peaks. For **5**, the four-peak pattern was the result of an overlap between the peaks due to one of the non-equivalent *ortho* carbons and one of the non-equivalent *meta* carbons. The latter case is exemplified in Fig. 2. In the case of **8** the four-peak pattern was the result of an overlap between the resonance from one of the nonequivalent *ortho* carbons and the *para* carbon.

For **16**, as the temperature was increased the *meta* carbon resonances coalesced and the *ortho* carbon resonances broadened. At the highest temperature which could be reached ( $140^\circ\text{C}$ ; due to apparatus limitations), the unsubstituted aromatic carbon region consisted of a sharp peak assigned to the *meta* carbons, a broad peak from the two *ortho* carbons beginning to overlap and a third peak from the *para* carbon.

The unsubstituted aromatic carbons in the  $^{13}\text{C}$  NMR spectra of **3**, **9** and **10** all showed three resolvable peaks at low temperature. For **10** the peaks were assigned as exemplified in Fig. 3—at lowest field one of the non-equivalent *ortho* carbons, then the two unresolved *meta* carbons and at highest field an overlap between the other *ortho* and the *para* carbon peaks. In the case of **9**, the *o'*-peak overlapped with

**Table 1.**  $^{13}\text{C}$  chemical shifts in neopentylbenzenes (in ppm) relative to TMS (at 28 °C)

Substance	Substituted aromatic	Unsubstituted aromatic	Benzylic	Quaternary <i>tert</i> -butyl	<i>tert</i> -Butyl	Other carbons	Solvent
1	137.1	130.0 ( <i>o</i> ) 127.0 ( <i>m</i> ) 124.8 ( <i>p</i> )	48.3	30.1	27.3	—	$\text{CHCl}_2\text{F}$
2	134.6	127.4 ( <i>o+p</i> ) 126.8 ( <i>m</i> )	104.7	33.7	23.1	$J = 21.5 \text{ Hz}$	$\text{CHCl}_2\text{F}$
3	135.6	125.6 ( <i>o</i> ) 124.9 ( <i>m+p</i> )	71.3	34.9	24.6	—	Acetone- $d_6$ - $\text{CS}_2$ (1:5)
4	136.1	124.6 ( <i>o</i> ) 123.3 ( <i>m</i> ) 123.0 ( <i>p</i> )	66.3	34.9	25.2	—	Acetone- $d_6$ - $\text{CS}_2$ (1:5)
5	137.7	125.2 ( <i>o</i> ) 123.5 ( <i>m</i> ) 123.2 ( <i>p</i> )	50.4	34.9	26.1	—	Acetone- $d_6$ - $\text{CS}_2$ (1:5)
6	144.6	128.3 ( <i>o</i> ) 128.0 ( <i>m</i> ) 127.7 ( <i>p</i> )	92.1	35.6	26.2	37.3 $\text{OCH}_3$	Acetone- $d_6$ - $\text{CS}_2$ (1:5)
7	136.3	125.1 ( <i>o+m+p</i> )	79.5	32.3	23.1	172.5 $\text{C}=\text{O}$ in $\text{CH}_3\text{CO}$ ; 18.7 $\text{CH}_3$ in $\text{CH}_3\text{CO}$	$\text{CHCl}_2\text{F}$
8	140.7	125.5 ( <i>m</i> ) 124.9 ( <i>o</i> ) 124.2 ( <i>p</i> )	79.6	33.5	23.1	-3.0 $\text{CH}_3$ in $\text{Si}(\text{CH}_3)_3$	$\text{CHCl}_2\text{F}$
9	145.3	129.1 ( <i>o</i> ) 127.9 ( <i>m</i> ) 126.1 ( <i>p</i> )	49.9	33.6	27.8	17.9 $\text{CH}_3$	$\text{CHCl}_2\text{F}$
10	143.8	129.8 ( <i>o</i> ) 128.1 ( <i>m</i> ) 126.4 ( <i>p</i> )	57.5	33.3	28.1	22.4 $\text{CH}_2$ in $\text{CH}_3\text{CH}_2$ ; 13.9 $\text{CH}_3$ in $\text{CH}_3\text{CH}_2$	Acetone- $d_6$ - $\text{CS}_2$ (1:5)
11	141.8	128.3 ( <i>o</i> ) 127.8 ( <i>m</i> ) 127.3 ( <i>p</i> )	81.8	34.6	26.2	—	Acetone- $d_6$
12	143.7	127.4 ( <i>o</i> ) 126.5 ( <i>m</i> ) 125.7 ( <i>p</i> )	77.1	37.6	25.4	24.1 $\text{CH}_3$	Acetone- $d_6$
13	142.0	128.1 ( <i>o</i> ) 126.9 ( <i>m</i> ) 125.9 ( <i>p</i> )	80.2	38.3	25.6	26.5 $\text{CH}_2$ in ethyl; 8.3 $\text{CH}_3$ in ethyl	Acetone- $d_6$
14	137.5	128.7 ( <i>o</i> ) 127.5 ( <i>m</i> ) 126.6 ( <i>p</i> )	76.8	34.8	25.7	37.1 $\text{CH}_2\text{CO}$ in butyl; 26.4 $\text{CH}_2-\text{CH}_2\text{CO}$ in butyl; 24.2 $\text{CH}_2(\text{CH}_2)_2\text{CO}$ in butyl; 14.0 $\text{CH}_3$ in butyl	Acetone- $d_6$
15	146.7	127.2 ( <i>m</i> ) 126.4 ( <i>o</i> ) 125.5 ( <i>p</i> )	80.8	38.6	27.7	34.1 $\text{CH}$ in isopropyl; 20.2 $\text{CH}_3$ in isopropyl; 19.1 $\text{CH}_3$ in isopropyl	$\text{DMSO-}d_6$ -acetone- $d_6$ (4:1)
16	146.8	129.0 ( <i>m</i> ) 128.8 ( <i>m</i> ) 128.3 ( <i>o</i> ) 127.0 ( <i>o+p</i> )	82.6	41.3	29.8	—	$\text{DMSO-}d_6$

the two unresolved *meta* carbon peaks, but in the case of **3** only the two non-equivalent *ortho* carbons were resolvable and the two *meta* and the *para* carbon peaks overlapped to give a broad band.

The low-temperature spectrum of **15** showed two peaks in the ratio 3:2 from the unsubstituted aromatic carbons (see Fig. 4). This pattern was assigned as an overlap between one of the two non-equivalent *ortho* carbons and the two unresolved *meta* carbons, and an overlap between the other *ortho* and the *para* carbon peaks.

The unsubstituted aromatic region in the  $^{13}\text{C}$  NMR spectrum of **7** at low temperature also consisted of two resolvable peaks (one broad) with an intensity ratio of 4:1. The small peak to high field was assigned to one

of the non-equivalent *ortho* carbons, and the broad peak was assigned as an overlap of the signals from all the other unsubstituted aromatic carbons.

The low-temperature chemical shifts for the unsubstituted aromatic carbons relative to the *para* carbon shift are given in Table 2 for compounds **3–10** and **12–16**.

**Band shape analysis.** The neopentyl group rotation is a two-site exchange between two identical sites (see Discussion). The temperature dependence of the aromatic  $^{13}\text{C}$  NMR spectra has consequently been simulated as two-site exchanges. For compounds **3** and **7**, only the resonances from the *ortho* carbons showed the expected temperature dependence, whereas for

## BARRIERS IN NEOPENTYLBENZENES

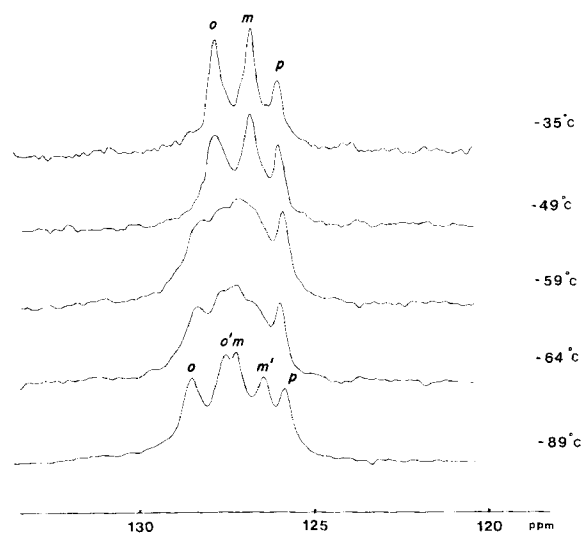


Figure 1. Unsubstituted aromatic carbons in the  $^{13}\text{C}$  NMR spectrum of compound **13** in acetone- $d_6$  solution at different temperatures.

**4-6, 8-10** and **12-16** both *ortho* and *meta* carbon resonances showed the expected temperature dependence at sufficiently low temperatures. In the latter cases, the spectra were treated as two overlapping two-site cases with an extra Lorentzian signal, from the *para* carbon, unaffected by the exchange.

For compounds **6, 9, 10** and **12-15** the *para* carbon signal was used as an internal resolution standard, whereas for **3-5** and **16** the benzylic carbon resonance was utilized for this purpose.

The rate constants obtained from the band shape

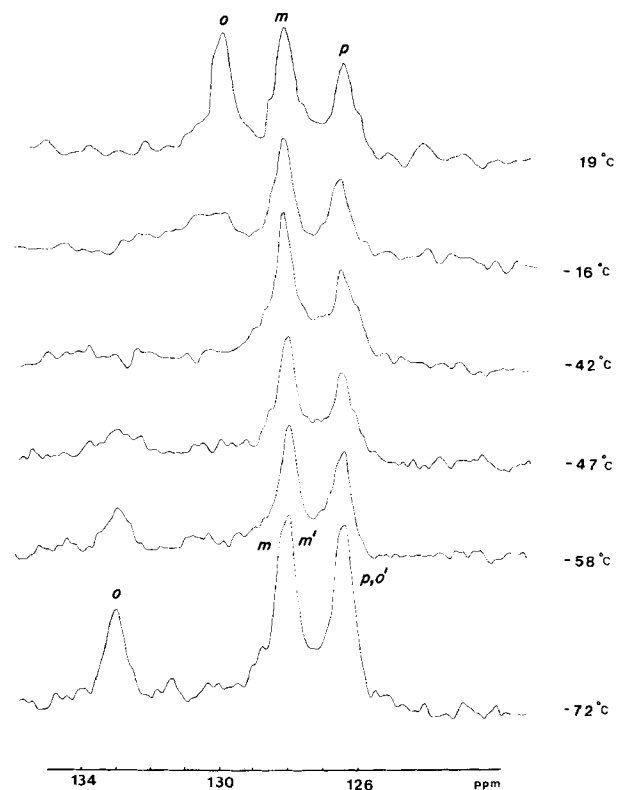


Figure 3. Unsubstituted aromatic carbons in the  $^{13}\text{C}$  NMR spectrum of compound **10** in  $\text{CS}_2$ -acetone- $d_6$  (5:1) solution at different temperatures.

analysis were used to calculate the free energy of activation ( $\Delta G_T^\ddagger$ ). The results are given in Table 3.

The entropy ( $\Delta S^\ddagger$ ) and enthalpy ( $\Delta H^\ddagger$ ) terms were also estimated for a few compounds from the temperature dependence of  $\Delta G_T^\ddagger$  (see Discussion, Table 7).

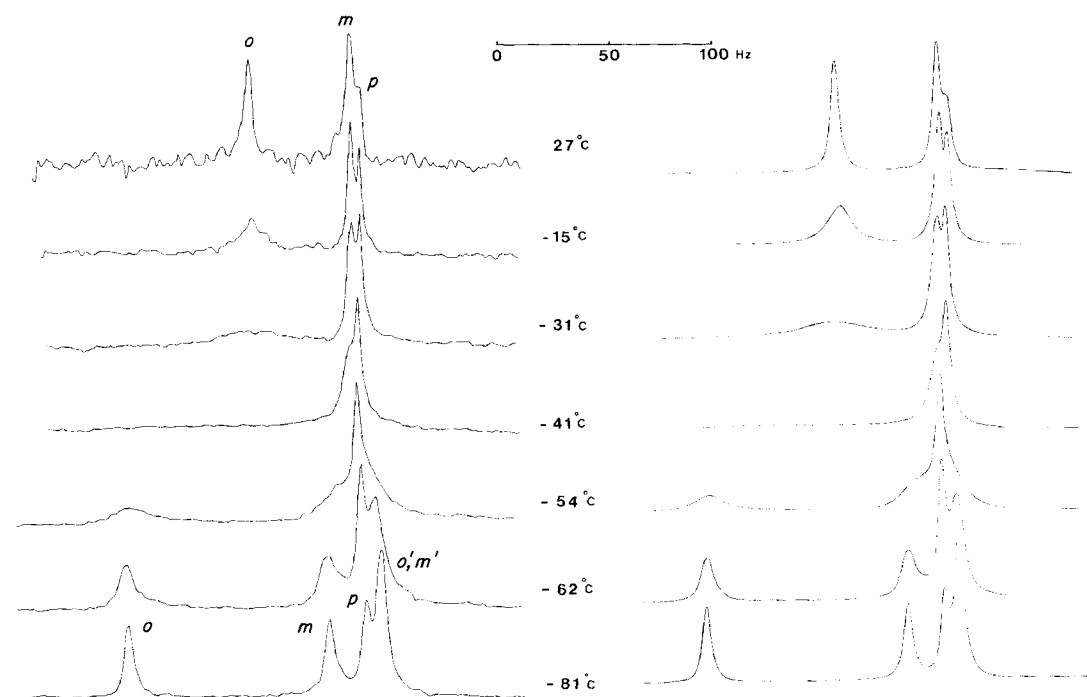
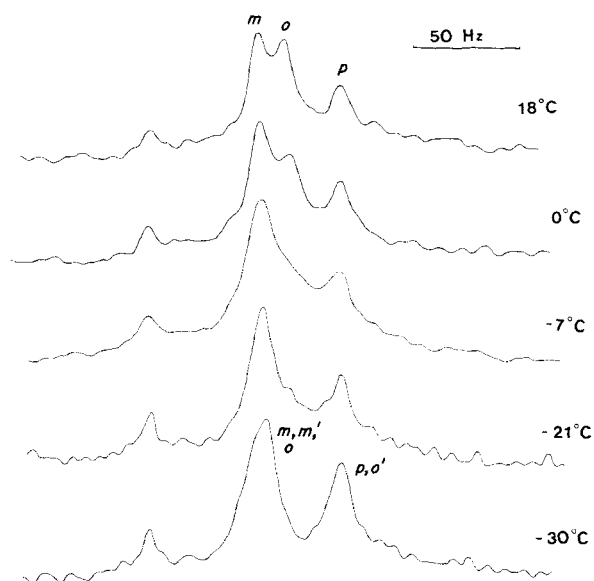


Figure 2. Unsubstituted aromatic carbons in the  $^{13}\text{C}$  NMR spectrum of compound **5** in  $\text{CS}_2$ -acetone- $d_6$  (5:1) solution at different temperatures (left) and iterated spectra (right).



**Figure 4.** Aromatic carbons in the  $^{13}\text{C}$  NMR spectrum of compound **15** in  $\text{DMSO-}d_6$ -acetone- $d_6$  (4:1) solution at different temperatures. The small peak to the left is from the substituted aromatic carbon.

### Rotation around the $\text{C}_{\text{sp}^3}$ - $\text{C}_{\text{sp}^3}$ bond

For all compounds except **1**, the *tert*-butyl resonance ( $^1\text{H}$  or  $^{13}\text{C}$ ) is expected to split into three signals of equal intensities for slow *tert*-butyl rotation, since the three methyl groups will then reside in different chemical environments. However, only for compounds **14**–**16** could three signals be resolved at a temperature low enough to slow down the *tert*-butyl rotation sufficiently (Fig. 5). In all other compounds, there was apparently accidental chemical shift equivalence between two of the three  $^{13}\text{C}$  methyl resonances, resulting in either a 1:2 or 2:1 doublet.

**Band shape analysis.** To estimate the *tert*-butyl rotation rate for **14**–**16** theoretical band shapes were calculated using a three-site exchange program. For all

**Table 2.** Low-temperature chemical shifts of unsubstituted aromatic carbons (ppm) relative to the *para*-carbon shift in some mononeopentylbenzenes<sup>a</sup>

Compound	<i>o</i>	<i>o'</i>	<i>m</i>	<i>m'</i>
<b>3</b>	1.1	0.5	0	0
<b>4</b>	2.2	0.9	0.6	-0.1
<b>5</b>	5.0	-0.3	0.7	-0.3
<b>6</b>	1.5	-0.4	0.6	0
<b>7</b>	1.3	-1.2	0	0
<b>8</b>	1.5	-0.1	1.6	1.0
<b>9</b>	4.3	1.8	1.9	1.8
<b>10</b>	6.5	0	1.6	1.6
<b>12</b>	2.0	1.6	1.0	0.7
<b>13</b>	2.7	1.7	1.4	0.6
<b>14</b>	2.5	1.6	1.2	0.6
<b>15</b>	1.6	0.2	1.7	1.6
<b>16</b>	1.3	0	2.0	1.8

<sup>a</sup> Shifts to high field relative to the *para*-carbon are given a negative sign.

**Table 3.**  $^{13}\text{C}$  chemical shift differences ( $\Delta\nu$ , between *ortho*- and *meta*-carbons, respectively) and free energies of activation ( $\Delta G_r^\ddagger$ ) for the neopentyl group rotation in some mononeopentylbenzenes

Compound	$\Delta\nu/\text{Hz}^a$	$\Delta G_r^\ddagger/\text{kJ mol}^{-1}$	( $T^\circ\text{C}$ ) <sup>b</sup>	Solvent
<b>3</b>	$16.0 \pm 1.5^c$	$36.0 \pm 0.9$	(-95)	Acetone- $d_6$ - $\text{CS}_2$ (1:5)
<b>4</b>	$32.8 \pm 1.5$	$40.9 \pm 1.0$	(-72)	Acetone- $d_6$ - $\text{CS}_2$ (1:5)
<b>5</b>	$17.6 \pm 1.5$	$46.5 \pm 0.7$	(-41)	Acetone- $d_6$ - $\text{CS}_2$ (1:5)
<b>6</b>	$26.0 \pm 1.0$	$46.2 \pm 0.5$	(-42)	Acetone- $d_6$ - $\text{CS}_2$ (1:5)
<b>7</b>	$63.0 \pm 2.0^c$	$36.1 \pm 1.6$	(-93)	$\text{CHCl}_2\text{F}$
<b>8</b>	$40.3 \pm 1.2$	$35.0 \pm 0.9$	(-102)	$\text{CHCl}_2\text{F}$
<b>9</b>	$15.0 \pm 1.2$	$39.2 \pm 0.5$	(-75)	$\text{CHCl}_2\text{F}$
<b>10</b>	$164.5 \pm 1.0$	$46.2 \pm 0.5$	(-42)	Acetone- $d_6$ - $\text{CS}_2$ (1:5)
<b>12</b>	$9.0 \pm 0.8$	$38.3 \pm 0.5$	(-89)	Acetone- $d_6$
<b>13</b>	$25.0 \pm 1.0$	$46.1 \pm 0.4$	(-59)	Acetone- $d_6$
<b>14</b>	$22.0 \pm 1.2$	$46.9 \pm 0.7$	(-53)	Acetone- $d_6$
<b>15</b>	$35.5 \pm 1.0$	$52.2 \pm 0.9$	(0)	Acetone- $d_6$ - DMSO- $d_6$ (1:4)
<b>16</b>	$32.8 \pm 1.0$	$90.5 \pm 1.0$	(138)	DMSO- $d_6$

<sup>a</sup> Errors in chemical shifts ( $\Delta\nu$ ) are estimated by changing  $\Delta\nu$  until a difference between calculated and measured spectra can be visually detected.

<sup>b</sup> Error in temperature  $\pm 2^\circ\text{C}$ .

<sup>c</sup> Only the shift difference between *ortho*-carbons could be estimated.

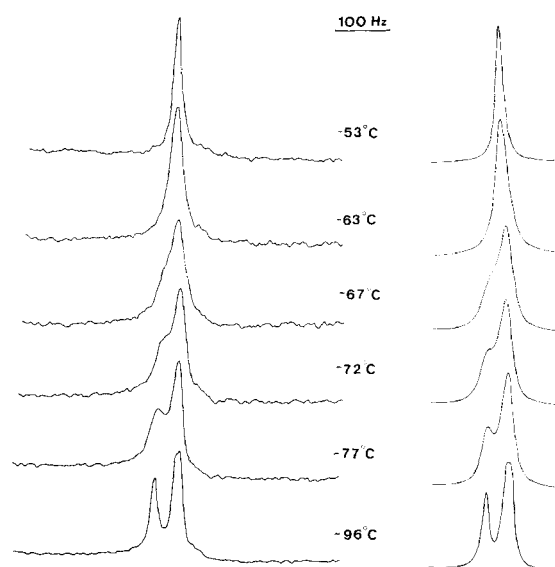


**Figure 5.** Temperature dependence of the methyl resonances in the *tert*-butyl group in the  $^{13}\text{C}$  NMR spectrum of compound **16** in  $\text{CHCl}_2\text{F}$  solution (left) and calculated spectra (right).

**Table 4.**  $^{13}\text{C}$  chemical shift differences ( $\Delta\nu$ ) and free energies of activation ( $\Delta G_T^\ddagger$ ) for the *tert*-butyl rotation in some mononeopentylbenzenes

Compound	$\Delta\nu/\text{Hz}^a$	$\Delta G_T^\ddagger/\text{kJ mol}^{-1}$	( $T/^\circ\text{C}$ ) <sup>d</sup>	Solvent
2	150.0±1.0	27.5±1.0	(-118)	$\text{CHCl}_2\text{F}$
3	215.0±1.0	32.4±0.5	(-100)	$\text{CHCl}_2\text{F}$
4	39.2 <sup>b</sup>	34.9±1.0	(-94)	Acetone- $d_6$ - $\text{CS}_2$ (1:4)
5	50.1 <sup>b</sup>	35.5±1.0	(-91)	Acetone- $d_6$ - $\text{CS}_2$ (1:4)
6	187.9±1.0	28.5±0.4	(-105)	$\text{CHCl}_2\text{F}$
7	144.4±1.0	27.5±0.6	(-114)	$\text{CHCl}_2\text{F}$
8	198.7±1.0	33.4±0.5	(-104)	$\text{CHCl}_2\text{F}$
9	221.0±2.0	26.4±0.5	(-119)	$\text{CHCl}_2\text{F}$
10	205.0±2.0	27.5±0.4	(-112)	$\text{CHCl}_2\text{F}$
12	65.0±1.5	31.8±0.6	(-99)	$\text{CHCl}_2\text{F}$
13	18.8 <sup>b</sup>	33.0±1.1	(-95)	$\text{CHCl}_2\text{F}$
14	15.0±1.0	36.0±0.9 <sup>c</sup>	(-91)	$\text{CHCl}_2\text{F}$
	14.9±1.0			
15	105.0±0.7	37.1±0.7 <sup>c</sup>	(-69)	$\text{CHCl}_2\text{F}$
	52.1±0.7			
16	36.0±0.7	41.1±0.6 <sup>c</sup>	(-63)	$\text{CHCl}_2\text{F}$
	10.0±0.7			

<sup>a</sup> Errors in chemical shifts ( $\Delta\nu$ ) were estimated by changing  $\Delta\nu$  until a clear difference between calculated and measured spectra could be visually detected.

<sup>b</sup> Estimated shift differences from broadenings just below coalescence, because low-temperature spectra could not be obtained owing to solubility problems or overlap from other signals.

<sup>c</sup> Exchange among three uncoupled sites.

<sup>d</sup> Error in temperature  $\pm 2^\circ\text{C}$ .

other compounds, the spectra were simulated as two-site exchanges with a 2:1 (or 1:2) population, and the rate constant of the low population site was used to calculate  $\Delta G_T^\ddagger$ . (This simplified treatment is justified since every  $120^\circ$  twist of the *tert*-butyl group will change the environment of the low population site, whereas only every second  $120^\circ$  twist will change the environment of the two carbons with the same shift.)

For all compounds except **8** the quaternary *tert*-butyl signal was used as a resolution standard; for **8** the  $\text{Si}(\text{CH}_3)_3$  signal was used for this purpose.

The free energy of activation ( $\Delta G_T^\ddagger$ ) was calculated from the estimated rate constants for all compounds, and the results are summarized in Table 4. For compound **15** the entropy and enthalpy terms were also estimated from the temperature dependence of  $\Delta G_T^\ddagger$  (see Discussion).

## DISCUSSION

### Neopentyl rotation

The calculated potential curve for neopentyl rotation in neopentylbenzene is shown in Fig. 6 (curve A). The curve (of height  $26.7\text{ kJ mol}^{-1}$ ) has a plateau-like shape, like that published for its 1,3,5-trisubstituted analogue (TNB).<sup>1h</sup> In this case the curve is, of course, completely symmetrical, in contrast to that of TNB.

Curve A in Fig. 6 shows a steep increase in steric energy when the dihedral angle  $\theta_{6178}$  (defined in the

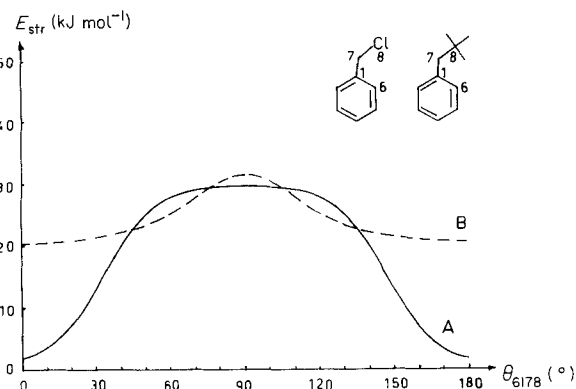


**Figure 6.** Calculated potential curves for internal  $\text{C}_{\text{sp}^3}\text{-C}_{\text{sp}^2(\text{arvl})}$  rotation in mononeopentylbenzene (curve A) and benzyl chloride (curve B). The dihedral angle  $\theta_{6178}$  is defined so that for values of  $0^\circ$  and  $180^\circ$  the substituent is perpendicular to the ring plane.

caption to Fig. 6) varies between  $15^\circ$  and  $60^\circ$ , since the *tert*-butyl group and two of its methyls (denoted \*) are forced to rotate when the phenyl group rotates (see below).

$\theta_{6178}/^\circ$	$\alpha/^\circ$	$\beta/^\circ$
0	60	58
20	62	50
40	67	38
60	72	16
80	66	13
90	60	15

When the angle  $\theta_{6178}$  changes from  $0^\circ$  to  $60^\circ$ , the *tert*-butyl group rotates by  $12^\circ$  ( $\alpha$  changes from  $60^\circ$  to  $72^\circ$ ), both methyl groups rotate by  $42^\circ$  ( $\beta$  changes from  $58^\circ$  to  $16^\circ$ ) and the steric energy increases drastically. When  $\theta_{6178}$  changes from  $60^\circ$  to  $90^\circ$ , the *tert*-butyl group rotates back into a staggered conformation ( $\alpha = 60^\circ$ ), while the two methyl groups remain essentially in the same twisted positions ( $\beta$  varies only between  $13^\circ$  and  $16^\circ$ ). The steric energy then remains essentially the same because the *tert*-butyl group rotates back into a staggered conformation.

MM calculations on benzyl chloride lead to a more peaked potential curve,  $10.7\text{ kJ mol}^{-1}$  in height (see curve B, Fig. 6). Curve B shows the greatest changes in steric energy when the dihedral angle  $\theta_{6178}$  varies between  $45^\circ$  and  $80^\circ$ . In this case, the greatest non-bonded interactions between the chlorine and ring hydrogens are found when  $\theta_{6178} = 90^\circ$ .

For both curves A and B, the initial state is calculated to be when the benzylic substituent (Cl or *t*-Bu) is perpendicular to the ring plane (conformer I, Fig. 7). In both cases, the transition state is found when the dihedral angle  $\theta_{6178} = 90^\circ$  (conformer III, Fig. 7).

The neopentyl barrier was found (above) to change from 36 to 41 to  $47\text{ kJ mol}^{-1}$  in neopentylbenzenes (A) when the substituent (X) changed from Cl to Br to I (Table 3). The barrier for the fluorine-substituted compound was too low to be measured.

A similar trend was found for the methyl rotation in benzyl (B) and benzal halides (C) by Schaefer *et*

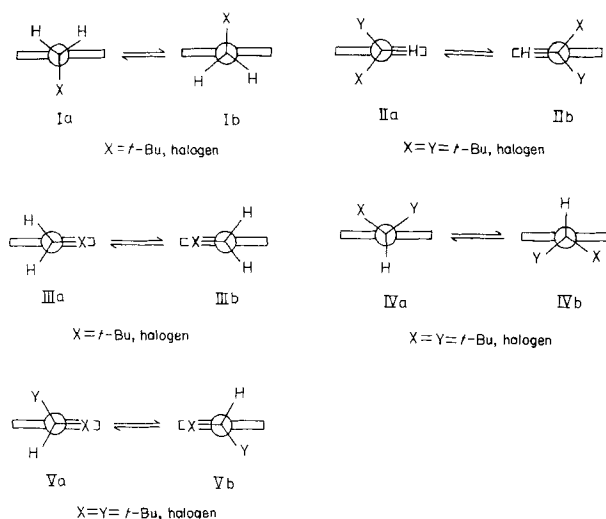
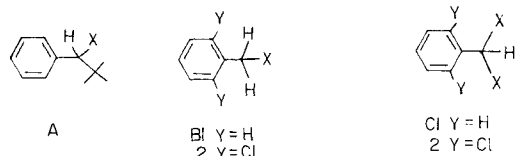
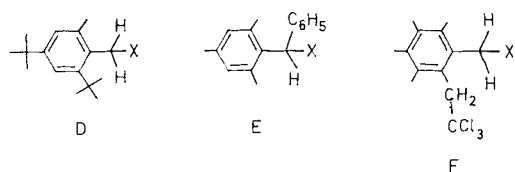


**Figure 7.** Different conformers for rotation around a benzylic bond (see text).

al.<sup>6a,8,15a-1</sup> from measurements of proton-proton (proton-fluorine) long-range coupling constants, and from DNMR measurements. Their results are given in Table 5, together with the results from measurements of torsional barriers in 2,4-di-*tert*-butyl-6-methylbenzyl halides (D) by Cupas *et al.*,<sup>16</sup> and those of



Manschreck and Ernst<sup>17a,b</sup> from their studies on internal rotation in toluenes (E). The results from dynamic NMR studies of 2-(2,2,2-trichloroethyl)-3,4,5,6-tetramethylbenzyl halides (F) by Elzinga and Hogeveen<sup>18</sup> are also presented.



When two benzylic substituents are present in the molecule, the potential curves in Fig. 6 can be used to give an indication of the nature of the initial and transition states. It is assumed that the effects from the potential curves in Fig. 6 are additive, which of course is a gross oversimplification. For two identical large groups, e.g. two *tert*-butyl groups, as benzylic substituents, the sum of two curves which are shifted 120° from each other will appear as shown in Fig. 8.

For the angle  $\theta = 30^\circ$  there is a minimum in the total potential curve. This conformation, which is the initial state, corresponds to conformer II in Fig. 7, i.e. the benzylic hydrogen lies in the ring plane. The transition state conformation occurs when  $\theta = 120^\circ$  (conformer IV in Fig. 7). The neopentyl barriers estimated according to Fig. 8 amount to *ca* 30 kJ mol<sup>-1</sup>. A comparison between Figs 6 (curve A) and 8 indicates that the neopentyl barrier is only slightly increased when a

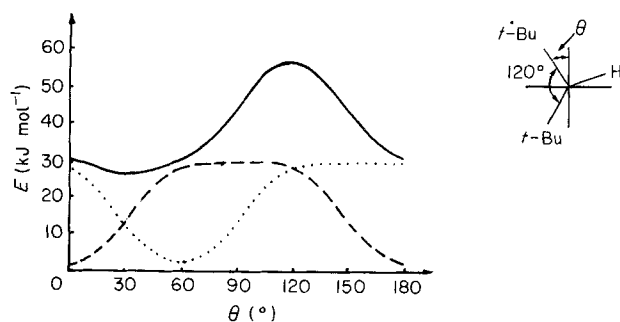
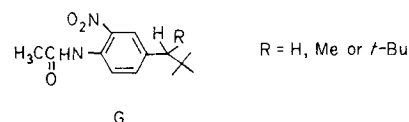


**Figure 8.** Total potential curve (—) for  $C_{sp^3}-C_{sp^2(aryl)}$  rotation and potential curves (---, ....) for two benzylic groups, separated by a 120° angle.

benzylic hydrogen in neopentylbenzene is replaced by a *tert*-butyl group. These theoretical results are not in agreement with experiment, which shows an increase in the neopentyl barrier of *ca* 70 kJ mol<sup>-1</sup>. Baas<sup>4a</sup> estimated a  $C_{sp^3}-C_{sp^2(aryl)}$  barrier for compound G



( $R = t\text{-Bu}$ ) to be 93 kJ mol<sup>-1</sup>, which is much greater than that indicated in Fig. 8. When  $R = H$ , Baas could not estimate the barrier, but the neopentyl barrier in TNB has been estimated to be *ca* 23 kJ mol<sup>-1</sup>.<sup>1d,g,h</sup> Thus, the neopentyl barrier in neopentylbenzene is probably <23 kJ mol<sup>-1</sup>. An explanation for these discrepancies may be that for a compound with two benzylic *tert*-butyls, the  $t\text{-Bu}-C_\alpha-t\text{-Bu}$  angle (where  $C_\alpha$  is the benzylic carbon), shown in Fig. 8, is greater than 120°, owing to steric interactions between the *tert*-butyl groups. The transition state energy may then increase as the *tert*-butyls are forced nearer the ring plane. The initial state energy may then decrease, as the *tert*-butyls are further from the ring plane in the initial state conformation, and the result may be a higher barrier to rotation.

When two benzylic chlorines are present in the molecule, Fig. 9 indicates that the initial state occurs when  $\theta = 30^\circ$  (conformer II in Fig. 7). The transition state occurs when  $\theta = 90^\circ$  or  $150^\circ$ , and these conformations correspond to conformer V in Fig. 7 (i.e. one chlorine lies in the ring plane). Fig. 9 also indicates that the energy in this conformer is only 2.5 kJ mol<sup>-1</sup>

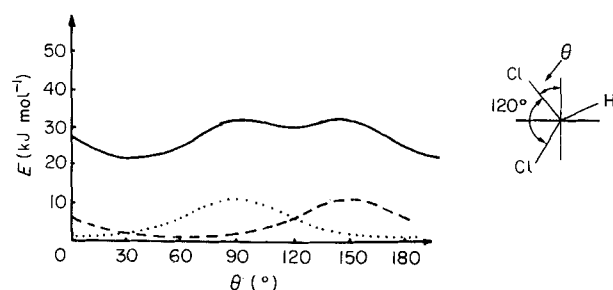


**Figure 9.** Total potential curve (—) for  $C_{sp^3}-C_{sp^2(aryl)}$  rotation, and potential curves (---, ....) for two benzylic chlorines, separated by a 120° angle.

greater than that in the conformer with  $\theta = 120^\circ$  (conformer IV in Fig. 7; this is probably within the error of the approximation). The simple considerations in Figs 8 and 9 indicate that even though both the dichloro- and di-*tert*-butyl-substituted compounds have the same initial state, they might not have the same transition states, owing to the plateau-like shape of the curve for the neopentyl group.

In compounds of types C1 and C2, Schaefer *et al.*<sup>8,15d-f,i-1</sup> proposed initial and transition states to be conformers II and V (Fig. 7), respectively. Schaefer *et al.*<sup>8,15c</sup> also proposed conformer IV (Fig. 7) to have lower energy than conformer V. However, in compounds of type H, Mannschreck and Ernst<sup>17b</sup> have found conformer IV to be the transition-state conformation. They also point out that, in performing such calculations, the entire molecule must be free to relax, which is, of course, of great importance.

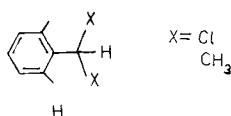
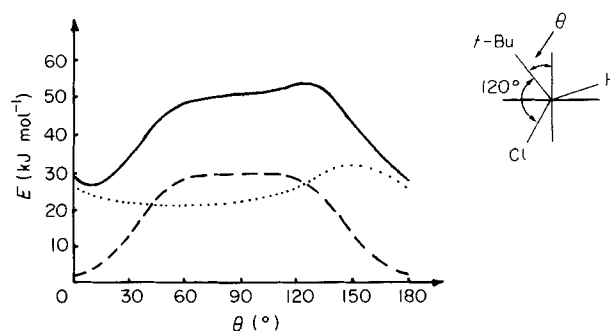


Figure 9 also indicates that the barrier in benzal chloride will be *ca* 10 kJ mol<sup>-1</sup>, i.e. comparable to the barrier calculated for benzyl chloride (11 kJ mol<sup>-1</sup>, curve B in Fig. 6). In this case the theoretical results are reasonable, and are in good agreement with the experimental results of Schaefer *et al.*,<sup>15g</sup> who found similar barriers for the molecular systems B1 and C1 when the substituent X was chlorine (Table 5).

If the two benzylic substituents are different in size, i.e. one is a chlorine and one is a *tert*-butyl group (as is the case for the systems studied here), Fig. 10 shows that the overall shape is very much dominated by the larger group, as expected. The minimum on the potential curve occurs when  $\theta = 10^\circ$ , and this initial state differs by only  $10^\circ$  from that for the case of the unsubstituted neopentyl group (conformer I, Fig. 7). Even though the perturbation of the potential curve due to the insertion of the chlorine is small, the maximum has shifted from  $\theta = 90^\circ$  to  $130^\circ$ , and the transition state differs by only  $10^\circ$  from that in the case of two benzylic *tert*-butyl groups (conformer IV, Fig. 7). The barrier to  $C_{sp^3}-C_{sp^2(aryl)}$  rotation indicated in Fig. 10 is 28 kJ mol<sup>-1</sup>, while the barrier experimentally estimated is 36.0 kJ mol<sup>-1</sup> (compound **3**, Table 3). The larger barrier to rotation found experimentally may be explained as the result of the *t*-Bu—C<sub>α</sub>—Cl angle in **3** being greater than  $120^\circ$  (as indicated in Fig. 10; cf. discussion of the compound in Fig. 8).

**Table 5. Measured  $C_{sp^3}-C_{sp^2(aryl)}$  rotational barriers (kJ mol<sup>-1</sup>) for different molecular systems (see text)**

Molecular system								
X	B	C1	C2	D1	D2	E	F	G
F	—	1.3	18.8	4.6	12.6	—	—	52.4
Cl	36.0	8.4	36.4	8.4	62.8	47.3	47.3	54.9
Br	40.9	13	44.8	14.7	77.0	52.3	53.2	56.9
I	46.5	15	50.7	—	87.9	66.6	—	59.5



**Figure 10.** Total potential curve (—) for  $C_{sp^3}-C_{sp^2(aryl)}$  rotation, and potential curves for a benzylic *tert*-butyl group (---) and a benzylic chlorine (...), separated by a  $120^\circ$  angle.

Initial and transition state conformations indicated in Fig. 10 are in good agreement with results from MM calculations on the neopentylbenzenes **9** and **10** with methyl and ethyl groups, respectively, as benzylic substituents. According to the calculations, the initial state conformations occur when  $\theta_{6178}$  is  $3^\circ$  (**9**) and  $8^\circ$  (**10**), i.e. the initial state is mostly defined by the larger of the two substituents (cf. conformer I, Fig. 7, X = *t*-Bu and one hydrogen replaced by Me or Et). The calculated transition states occur when  $\theta_{6178}$  is  $114^\circ$  (**9**) and  $120^\circ$  (**10**) (cf. conformer IV). The calculated neopentyl barriers are 54.2 and 65.4 kJ mol<sup>-1</sup> for **9** and **10**, respectively. The calculations also show that conformations corresponding to conformer V in Fig. 7 are 15 (**9**) and 24 (**10**) kJ mol<sup>-1</sup> more stable than the corresponding transition states. A similar result is also indicated in Fig. 10 (compound **3**). The *t*-Bu—C<sub>α</sub>—Me and *t*-Bu—C<sub>α</sub>—Et angles found from the calculations are  $125^\circ$  (**9**) and  $127^\circ$  (**10**) in the corresponding initial states, which provides support for the suggestion that the *t*-Bu—C<sub>α</sub>—Cl angle in compound **3** may in reality be larger than  $120^\circ$  in the initial state. In the transition states of compounds **9** and **10**, the calculations show that the *t*-Bu—C<sub>α</sub>—Me and *t*-Bu—C<sub>α</sub>—Et angles are in both cases  $120^\circ$ , which is indicated in Fig. 10.

The MMP1 program has been shown to give calculated barriers in TNB that are too high.<sup>1h</sup> When this work was in progress, the Allinger MMP2 program, which is more refined, became available to us.<sup>12</sup> Initial and transition states for compounds **9** and **10** were recalculated and gave the neopentyl barriers 40.3 (**9**) and 54.7 (**10**) kJ mol<sup>-1</sup>, which are in good agreement with those estimated experimentally (Table 3).

A comparison between Fig. 6 (curve A) and the approximate curve in Fig. 10 indicates that the neopentyl barrier will be the same whether or not a chlorine is introduced in the benzylic position in neopentylbenzene. This is in contrast to experimental results, since the barrier experimentally estimated for neopentylbenzene is  $<23$  kJ mol<sup>-1</sup> and that for compound **3** is 36 kJ mol<sup>-1</sup> (Table 3).

The theoretical results in Figs 8 and 10 indicate that the neopentyl barrier is essentially unaffected when a benzylic chlorine is replaced by a *tert*-butyl group. However, experimental results show that there is a large difference from 93 kJ mol<sup>-1</sup> (compound G, R = *t*-Bu) to 36 kJ mol<sup>-1</sup> (compound **3**, Table 3). It

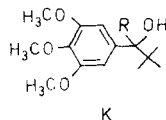
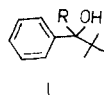
seems reasonable that the  $t\text{-Bu}-\text{C}_\alpha-\text{X}$  angle increases as the effective size of the substituent X increases, i.e. the larger the  $t\text{-Bu}-\text{C}_\alpha-\text{X}$  angle the larger is the barrier to rotation.

The curves in Fig. 6 also make it possible to construct potential curves when three benzylic substituents are present in the molecule.<sup>19</sup> These curves indicate that the neopentyl barriers for the compounds in Figs 8 and 10 decrease when a  $t\text{-Bu}$  or a Cl group replaces the benzylic hydrogen. These results are in qualitative agreement with experiments by Anderson *et al.*,<sup>20</sup> who found the neopentyl barrier in  $p\text{-NO}_2(\text{OCH}_3)$ -substituted **9** decreased by 5.0 (5.8)  $\text{kJ mol}^{-1}$  when the benzylic proton was replaced by a chlorine.

**Comments on the results for compounds 6-8.** When the substituent is acetate or trimethylsilyloxy (compounds **7** and **8**), the measured neopentyl barriers ( $\Delta G_T^\ddagger$ ) are 36.1 and 35.0  $\text{kJ mol}^{-1}$ , respectively (Table 3), but when the substituent is a methoxy group (compound **6**) the barrier is 40.2  $\text{kJ mol}^{-1}$ . These results can be explained by the 'flatness' of the carbonyl part of the acetate group, and this part probably orients perpendicularly to the benzylic bond. The steric hindrance caused by the benzylic acetate group in **7** should then be less than that caused by the methoxy group in **6**.

For silyl ethers, Si—O bond lengths of  $1.633 \pm 0.005 \text{ \AA}$  are commonly quoted in the literature,<sup>21a,b</sup> while those for O—CH<sub>3</sub> ethers are  $1.435 \pm 0.005 \text{ \AA}$ .<sup>21a</sup> The same relative bond lengths will probably exist for benzylic substitution, and thus the longer O—Si bond will make the Si(CH<sub>3</sub>)<sub>3</sub> group in **8** be further from the benzylic position than the CH<sub>3</sub> group in **6**, thus alleviating the steric hindrance.

**Compounds 11-16.** A large effect on the  $\Delta G_T^\ddagger$  values for the  $\text{C}_{\text{sp}^3}-\text{C}_{\text{sp}^2(\text{aryl})}$  rotation is observed in compounds of type I when one of the two benzylic substituents is varied (Table 3). The results are compared with those from <sup>1</sup>H NMR spectroscopic studies<sup>46</sup> of the  $\text{C}_{\text{sp}^3}-\text{C}_{\text{sp}^2(\text{aryl})}$  rotation in 1-hydroxy-1-alkyl-1-(3,4,5-trimethoxyphenyl)-2,2-dimethylpropanes (K, Table 6).



When the substituent  $\text{R}=\text{H}$  in the I series, the barrier could not be estimated by <sup>13</sup>C NMR spectroscopy, probably owing to shift equivalence. There is very good agreement between the estimated neopentyl barriers in series I and K (Table 6). It should be noted, however, that the measurements were not performed in the same solvent, except for the case of  $\text{R}=\text{t-Bu}$ , where DMSO-*d*<sub>6</sub> was used as solvent in both cases.

When two *tert*-butyls are benzylic substituents, Fig. 8 indicates conformer II (Fig. 7) to be the initial state. This conformation will probably remain as the initial state when the benzylic proton is replaced by a hydroxyl group, since the *tert*-butyls are much larger in size. This conformation, with the hydroxyl group in the ring plane, was also proposed by Baas *et al.*<sup>4b</sup> and

**Table 6. Barriers to internal  $\text{C}_{\text{sp}^3}-\text{C}_{\text{sp}^2(\text{aryl})}$  rotation ( $\text{kJ mol}^{-1}$ ) for some benzylic alcohols (see text)**

Molecular system		
R	I	K
H	—	36.4±1.2
Me	38.3±0.5	39.4±1.2
Et	46.1±0.4	47.3±1.2
<i>n</i> -Pr	—	47.3±1.2
<i>n</i> -Bu	46.9±0.7	47.7±1.2
<i>i</i> -Pr	52.2±0.9	54.4±1.2
<i>t</i> -Bu	90.5±1.0	89.6±1.2 <sup>a</sup>

<sup>a</sup> Gall *et al.*<sup>5a</sup> estimated  $\Delta G^\ddagger = 86-94 \text{ kJ mol}^{-1}$  for this compound in DMSO-*d*<sub>6</sub> solution.

Gall *et al.*<sup>5a</sup> in their <sup>1</sup>H NMR spectroscopic studies to be the initial state for the alcohol with two benzylic *tert*-butyl groups.

Baas *et al.*<sup>4b</sup> thought it to be very probable that the initial state conformation proposed for the di-*tert*-butyl alcohol will also be the same when one of the two benzylic *tert*-butyl groups is replaced by an *n*-Bu or an Et group. On the other hand, when one of the benzylic *tert*-butyl groups is replaced by an H or a Me group, they thought the initial state to be different. A possible initial state conformation proposed in these cases was one in which the H or the Me group was in the ring plane. MM calculations on neopentylbenzenes with Me and Et as benzylic substituents, and without hydroxyls (compounds **9** and **10**), have shown that initial and transition states are rather similar in both cases. ( $\theta_{6178}$  defined in Fig. 6 differs by 3° between the initial states and by 6° between the transition states). This similarity will probably remain when benzylic hydroxyl groups are introduced in these compounds.

Gall *et al.*<sup>5a</sup> suggested a transition state conformation for 3,4,5-trisubstituted phenyl di-*tert*-butyl carbinols where one of the two *tert*-butyl groups passes the ring plane (conformer V; Fig. 7). This suggestion was based on inspection of models and no calculations were made. As pointed out at the beginning of this discussion (Fig. 8), such a transition state conformation has lower energy than a conformation where  $\theta = 120^\circ$  (conformer IV, Fig. 7) when the benzylic substituents are two *tert*-butyl groups. Probably both the initial and transition states will be the same when the benzylic H is replaced by an OH group, because this group is much smaller than the two benzylic *tert*-butyl groups. MM calculations, although on compounds where only one of the benzylic substituents is a *tert*-butyl group (compounds **9** and **10**), have shown that a conformer in which  $\theta_{6178}$  (Fig. 6) is 90° has a lower energy than the transition state conformations. It is therefore more probable that conformer IV will correspond to the transition state conformation in the case of **16**.

The experimental barrier to internal neopentyl rotation found for **13** is (within the limits of error) the same as that for **14** (Table 3). The steric strain caused by the *n*-Bu group in **14** is thus probably the same as

that due to the ethyl group in **13**. A similar trend was also found in the K series.<sup>4b</sup>

Comparison of the neopentyl barriers found for the alcohols (**12–16**, Table 3) also shows that the difference in  $\Delta G_T^\ddagger$  values between **13** and **15** is smaller than that between **15** and **16**. A moderate increase in the neopentyl barrier of  $6.1 \text{ kJ mol}^{-1}$  is found when one proton on the  $\text{CH}_2$  carbon in the ethyl group in **13** is replaced by a methyl group. On the other hand, when the methine proton in the isopropyl group in **15** is replaced by a methyl group, an increase in the neopentyl barrier of  $38.3 \text{ kJ mol}^{-1}$  is found. Baas *et al.*<sup>4b</sup> also found a similar trend in the K series. They explained this difference in the following manner, which may also be applicable to the I series: 'Consider the strain present in the system  $\text{R}-\text{C}_\alpha-t\text{-Bu}$  ( $\text{C}_\alpha$  is the benzylic carbon), especially for  $\text{R}=t\text{-Bu}$ . In the initial state the groups R and  $t\text{-Bu}$  will be bent outwards. This outward bending will diminish the angle  $\text{Ph}-\text{C}_\alpha-t\text{-Bu}$  and, thus, will increase the repulsive interactions in the transition state. Moreover, the steric strain in the transition state between the *tert*-butyl group and the *ortho*-carbon and hydrogen atoms of the benzene ring will diminish if the phenyl and *tert*-butyl groups bend away from each other. The latter outward bending will be more difficult with the increase in the strain between the *tert*-butyl group and the R group.'

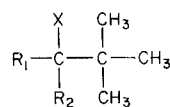
The activation parameters  $\Delta H^\ddagger$  and  $\Delta S^\ddagger$  for internal neopentyl rotation were estimated for a few compounds (see Table 7). The  $\Delta H^\ddagger$  and  $\Delta S^\ddagger$  values found for **4**, **5** and **9** are in good agreement with those estimated by Nilsson *et al.*<sup>1d</sup> for the neopentyl rotation in 2,4-dibromo-, 2,4-diiodo- and 2,4-dimethyl-TNB. However, it must be borne in mind that the compounds were not measured in the same solvent, and even though it is difficult to estimate accurate entropies from NMR measurements, the  $\Delta S^\ddagger$  term is known<sup>22</sup> to be sensitive to the medium.

### $\text{C}_{\text{sp}^3}-\text{C}_{\text{sp}^3}$ rotation

For compounds **2–8** and **12–16** the steric hindrance to internal *tert*-butyl rotation increases as the bulkiness of the benzylic substituent increases (cf. Table 4). Studies on *tert*-butyl rotations are not as frequently found in the literature as those for  $\text{C}_{\text{sp}^3}-\text{C}_{\text{sp}^2(\text{aryl})}$  rotations, but papers have appeared by Hawkins *et al.*<sup>23</sup> and Anderson and Pearson<sup>24a–e</sup> on halogen-substituted ethanes L and M. Freitag and Schneider<sup>25</sup> studied 2-substituted 3,3-dimethylbutanes N by  $^1\text{H}$  NMR spectroscopy. They also carried out MM calculations with the Allinger MM1 program on substituted neopentanes O. Bushweller and Anderson<sup>26</sup> have

**Table 7.** Activation parameters  $\Delta H^\ddagger$  ( $\text{kJ mol}^{-1}$ ) and  $\Delta S^\ddagger$  ( $\text{J mol}^{-1} \text{K}^{-1}$ ) for the neopentyl rotation in some neopentylbenzenes

Compound	$\Delta H^\ddagger$	$\Delta S^\ddagger$	Solvent
<b>4</b>	$40.2 \pm 2.6$	$-7 \pm 13$	Acetone- $d_6$ - $\text{CS}_2$ (1:5)
<b>5</b>	$44.5 \pm 1.9$	$-10 \pm 8$	Acetone- $d_6$ - $\text{CS}_2$ (1:5)
<b>9</b>	$37.6 \pm 3.3$	$-8 \pm 16$	$\text{CHCl}_2\text{F}$
<b>10</b>	$43.4 \pm 2.0$	$-13 \pm 9$	Acetone- $d_6$ - $\text{CS}_2$ (1:5)



L: X = halogen  $\text{R}_1 = \text{Cl}$   $\text{R}_2 = \text{H}$  or alkyl

" "  $\text{R}_1 = \text{Br}$  "

M: "  $\text{R}_1 = \text{CH}_3$  "

N: "  $\text{R}_1 = \text{H}$   $\text{R}_2 = \text{CH}_3$

O: "  $\text{R}_1 = \text{R}_2 = \text{H}$

P: X =  $\text{R}_1 = \text{H}$  or alkyl  $\text{R}_2 = \text{alkyl}$

R: X = halogen or alkyl  $\text{R}_1 = \text{C}_6\text{H}_5$

$\text{R}_2 = \text{H}$

studied various alkyl-substituted ethanes P. The results from Refs 23, 24a–e and 25 are compared with those from the neopentylbenzene system R in Table 8.

Table 8 shows excellent agreement in trends between the R series and the other series. Estimated *tert*-butyl barriers for neopentylbenzenes show a tendency to increase as the effective size of the halogen substituent increases. The initial and transition states are, of course, the staggered and eclipsed conformations, respectively. These conformations have also been proposed by Anderson and Pearson<sup>24a–c</sup> and by Hawkins *et al.*<sup>23</sup>

The *tert*-butyl barriers estimated for the neopentylbenzenes with benzylic methyl and ethyl groups (compounds **9** and **10**, respectively) are nearly the same, within experimental error (see Table 4). Bushweller and Anderson<sup>26</sup> also observed that the *tert*-butyl barrier in ethanes where the substituted carbon has one proton left (molecular system P) was nearly unchanged (within experimental error) as the bulkiness of the alkyl group substituent increased. This seems to indicate that<sup>26</sup> the initial state energy increases (owing to steric interactions) as much as that of the transition state when the bulkiness of the substituent increases.

For compounds **12–16**, where the benzylic carbon is quaternary, an increase in the *tert*-butyl barrier is found as the size of substituent increases:

Substituent:	Me	Et	<i>n</i> -Bu	<i>i</i> -Pr	<i>t</i> -Bu
$\Delta G_T^\ddagger$ ( $\text{kJ mol}^{-1}$ ):	$31.8 \pm 0.6$	$33.0 \pm 1.1$	$36.0 \pm 0.9$	$37.1 \pm 0.7$	$41.1 \pm 0.6$

A similar trend in the *tert*-butyl barrier was found by Anderson and Pearson<sup>24d,e</sup> when  $\text{X} = \text{Cl}$ ,  $\text{R}_1 = \text{alkyl}$  and  $\text{R}_2 = \text{CH}_3$  in the molecular structure M above. When  $\text{R}_1$  varied from Me to Et and *t*-Bu the  $\Delta G^\ddagger$  value for internal *tert*-butyl rotation was found to change from 44 to 45 and 49  $\text{kJ mol}^{-1}$ , respectively.

Only for compound **15** could the activation parameters be estimated. The enthalpy found is  $39.6 \pm$

**Table 8.** Barriers to internal *t*-butyl rotation ( $\Delta G^\ddagger$  in  $\text{kJ mol}^{-1}$ ) for different molecular systems (see text)

X	Molecular system					
	L ( $\text{R}_2 = \text{CH}_3$ )		M ( $\text{R}_2 = \text{CH}_3$ )	N	O	R
	$\text{R}_1 = \text{Cl}$	$\text{R}_1 = \text{Br}$	$\text{R}_1 = \text{CH}_3$			
H	—	—	29.2	20.5	15.1 <sup>a</sup>	—
F	—	—	33.7	—	—	27.5
Cl	45.3	49.8	43.7	32.2	21.3 <sup>a</sup>	32.4
Br	49.8	51.4	44.9	32.7	21.2 <sup>a</sup>	34.9
I	—	—	46.6	—	22.8 <sup>a</sup>	35.5
$\text{CH}_3$	41.1	45.2	—	28.1	16.1 <sup>a</sup>	26.4

<sup>a</sup> Values from MM calculations with the Allinger MM1 program.

2.2 kJ mol<sup>-1</sup> and the entropy 9 ± 11 J mol<sup>-1</sup> K<sup>-1</sup>, i.e. the ΔS<sup>‡</sup> value cannot be distinguished from zero.

### The size of the methyl group

From the experimentally estimated C<sub>sp<sup>3</sup></sub>-C<sub>sp<sup>2</sup>(aryl)</sub> barriers (Table 3) in α-Cl, -CH<sub>3</sub> and -Br-substituted neopentylbenzenes, the order of relative sizes Cl < CH<sub>3</sub> < Br can be estimated. This trend has also been found in ring-substituted TNB compounds.<sup>1d</sup> From estimated C<sub>sp<sup>3</sup></sub>-C<sub>sp<sup>3</sup></sub> barriers (Table 4) the order CH<sub>3</sub> < Cl < Br can be deduced, which is in agreement with results from substituted ethanes (see Table 8). This illustrates the points made by Nilsson *et al.*<sup>1d</sup> and Hounshell *et al.*,<sup>27</sup> namely that the trends depend on the molecular system involved and that the methyl, chloro and bromo groups are not strictly comparable. The chloro and bromo groups have local C<sub>∞v</sub> (conical) symmetry, i.e. they are 'pear shaped,' whereas the methyl group has local C<sub>3v</sub> symmetry, i.e. it is 'three pronged.'<sup>27</sup>

### CONCLUSIONS

Summations of calculated potential curves for α-substituted toluenes are of great value in order to predict conformations for α, α-disubstituted and α,α,α-trisubstituted toluenes. The results show that in the case of different α-substituents, as in C<sub>6</sub>H<sub>5</sub>CH(Cl)(*t*-Bu), the potential curve is very much dominated by the curve for the larger of the substituents (compound C<sub>6</sub>H<sub>5</sub>CH<sub>2</sub>-*t*-Bu). Initial and transition states for C<sub>6</sub>H<sub>5</sub>CH(Cl)(*t*-Bu) are, of course, also close to those calculated for C<sub>6</sub>H<sub>5</sub>CH<sub>2</sub>-*t*-Bu. MM calculations on C<sub>6</sub>H<sub>5</sub>CH(Me)(*t*-Bu) and C<sub>6</sub>H<sub>5</sub>CH(Et)(*t*-Bu) confirm these predictions.

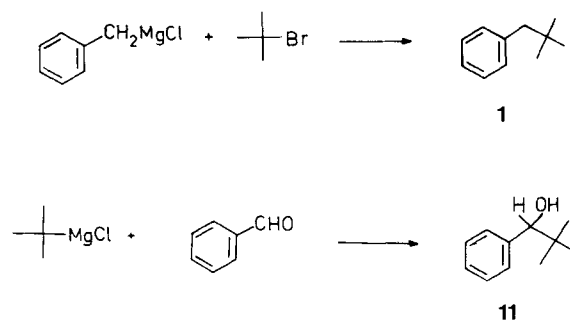
However, predictions of the height of the barrier to C<sub>sp<sup>3</sup></sub>-C<sub>sp<sup>2</sup>(aryl)</sub> rotation may not be straightforward, because the summations are based on the approximation that the angle X-C<sub>α</sub>-X (where C<sub>α</sub> is the benzylic carbon) is 120°. MM calculations confirm that the angle X-C<sub>α</sub>-X is different in the initial and transition states and may deviate considerably from 120°. These observations may explain why barriers from summed potential curves deviate considerably from those experimentally estimated when the substituents are large (X = *t*-Bu), but good agreement is found when the substituents are smaller (X = Cl).

Two orders of relative sizes (Cl < CH<sub>3</sub> < Br and CH<sub>3</sub> < Cl < Br) could be deduced from estimated C<sub>sp<sup>3</sup></sub>-C<sub>sp<sup>2</sup>(aryl)</sub> and C<sub>sp<sup>3</sup></sub>-C<sub>sp<sup>3</sup></sub> barriers, respectively. Thus, the relative size of a methyl group in relation to chlorine and bromine atoms is not independent of the system studied.<sup>1d,27</sup>

### SYNTHESES

Neopentylbenzene (**1**) was synthesized from benzylmagnesium chloride and *tert*-butyl bromide according to Bygdén.<sup>28</sup>

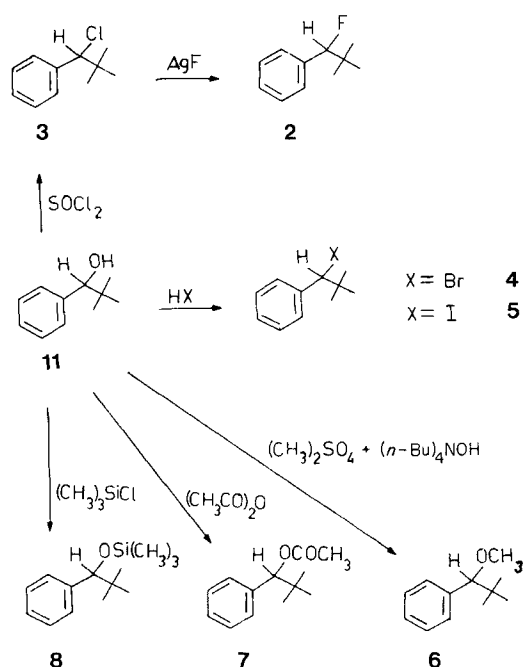
1-Hydroxy-2,2-dimethylpropylbenzene (**11**)<sup>29</sup> was synthesized from benzaldehyde and *tert*-butylmagnesium chloride, and was used as the starting material for the synthesis of compounds **3-8**.

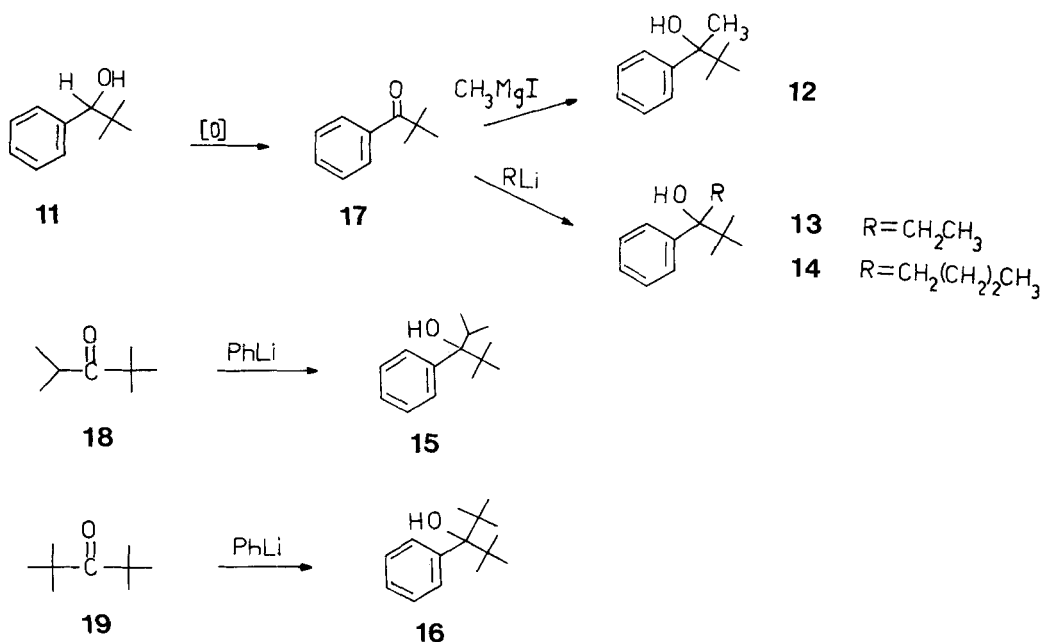


The reaction between **11** and appropriate reagents, such as thionyl chloride, hydrogen bromide and hydrogen iodide, afforded the compounds 1-chloro-2,2-dimethylpropylbenzene (**3**), 1-bromo-2,2-dimethylpropylbenzene (**4**) and 1-iodo-2,2-dimethylpropylbenzene (**5**), respectively. Reaction of **3** with silver fluoride in acetonitrile gave 1-fluoro-2,2-dimethylpropylbenzene (**2**).

1-Methoxy-2,2-dimethylpropylbenzene (**6**) was prepared from **11** by reaction with dimethyl sulphate under phase transfer catalysis conditions.<sup>30</sup> 1-Acetoxy-2,2-dimethylpropylbenzene (**7**) and 1-trimethylsilyloxy-2,2-dimethylpropylbenzene (**8**) were prepared by reaction between **11** and acetic anhydride in pyridine and trimethylsilyl chloride in pyridine, respectively.

2-Phenyl-3,3-dimethylbutan-2-ol (**12**), 3-phenyl-2,2-dimethylpentan-3-ol (**13**) and 3-phenyl-2,2-dimethylheptan-3-ol (**14**) were prepared by the reaction between pivalophenone [phenyl *tert*-butyl ketone, (**17**)] and the appropriate metal organic reagents: methylmagnesium iodide, ethyllithium and *n*-butyllithium, respectively. Pivalophenone (**17**) was prepared by oxidation of **11**.<sup>31a,b</sup> Reaction between





phenyllithium and the ketones 2,2,4-trimethylpentan-3-one [*tert*-butyl isopropyl ketone (**18**)]<sup>32a,b</sup> and 2,2,4,4-tetramethylpentan-3-one [*di-tert*-butyl ketone (**19**)]<sup>33,34</sup> gave the alcohols 3-phenyl-2,2,4-trimethylpentan-3-ol (**15**) and 3-phenyl-2,2,4,4-tetramethylpentan-3-ol (**16**), respectively.

3-Phenyl-2,2-dimethylbutane (**9**) and 3-phenyl-2,2-dimethylpentane (**10**) were prepared by hydration of 2-phenyl-3,3-dimethylbutene [ $\alpha$ -*tert*-butylstyrene (**20**)] and the olefin mixture *Z*- and *E*-3-phenyl-4,4-dimethylpent-2-ene (**21**+**22**), respectively. These olefins were synthesized by reaction between **17** and triphenylmethylenephosphorane or triphenylethylidenephosphorane.

### Preparative

<sup>1</sup>H NMR spectra for identification were run on a JEOL JNM 60 spectrometer. The chemical shifts are reported in ppm downfield from tetramethylsilane. The multiplicities of the peaks are designated as a singlet (s), doublet (d), triplet (t), quartet (q) and multiplet (m).

The IR spectra were run on a Perkin-Elmer 257 grating infrared spectrometer using sodium chloride cells.

The mass spectra were determined on an LKB MS 9000 mass spectrometer operating with 70 eV electron energy and situated at the University of Lund.

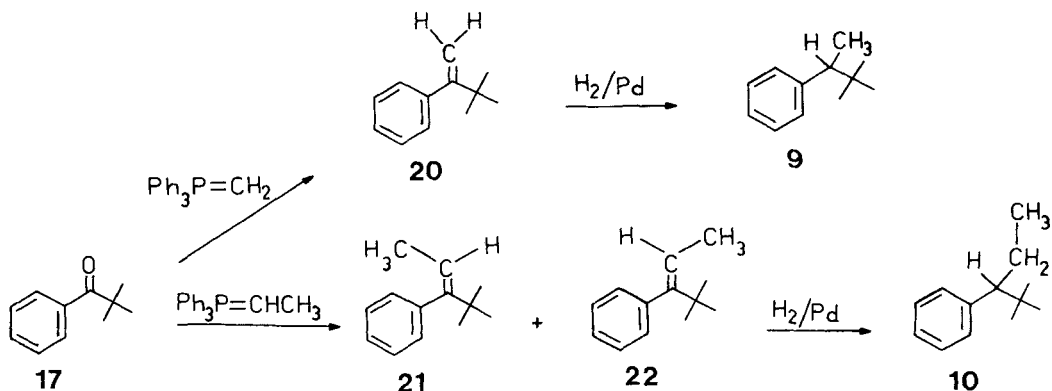
Elemental analyses were performed by the Analytical Service Laboratory at the University of Lund.

The gas-liquid chromatographic (GLC) analyses were carried out on a Varian Aerograph 1400 gas chromatograph with a 2 m  $\times$   $\frac{1}{8}$  in. o.d. column. The stationary phase was 3% SE-30 silicone gum rubber on Chromosorb G, and the flow-rate of the carrier gas (nitrogen) was 25 ml/min.

*Neopentylbenzene* (**1**). B.p. 91–92 °C/38 Torr,  $n_D^{24}$  = 1.4882 (lit.<sup>28</sup> b.p. 185.6–186.0 °C/757.6 Torr,  $n_D^{18}$  = 1.48837).

1-Hydroxy-2,2-dimethylpropylbenzene (**11**). B.p. 97–98 °C/9 Torr (lit.<sup>29</sup> b.p. 95 °C/7 Torr).

1-Chloro-2,2-dimethylpropylbenzene (**3**). Thionyl chloride (8.7 g, 73.2 mmol) was added to 1-hydroxy-2,2-dimethylpropylbenzene (4.0 g, 24.4 mmol) in a round-bottomed flask. The reaction mixture was stirred for 4 h at room temperature and was then poured into 30 ml of ice-water. The aqueous phase was extracted three times with 10 ml of diethyl ether. The organic phases were collected, dried (MgSO<sub>4</sub>), the ether was evaporated and the residue distilled in vacuum to give 3.7 g of a colourless liquid, yield 82%, b.p. 87–88 °C/6 Torr,  $n_D^{25}$  = 1.5146 (lit.<sup>35</sup> b.p. 89.5–



90.5 °C/6.7 Torr,  $n_D^{25} = 1.5142$ ).  $^1\text{H NMR}$  ( $\text{CDCl}_3$ ):  $\delta$  1.04 [9H, s,  $\text{C}(\text{CH}_3)_3$ ], 4.76 (1H, s, CH), 7.33 (5H, m, arom. H).

**1-Fluoro-2,2-dimethylpropylbenzene (2).** 1-Chloro-2,2-dimethylpropylbenzene (9.0 g, 49.4 mmol) was dissolved in 20 ml of dry acetonitrile. Anhydrous silver fluoride (9.4 g, 74.2 mmol) was added and the reaction mixture was refluxed for 10 h with stirring. After cooling, the reaction mixture was filtered, the solvent evaporated, 20 ml of water were added and the aqueous phase was extracted three times with 10 ml of cyclohexane. The organic phases were collected, dried ( $\text{MgSO}_4$ ), the solvent was evaporated and the residue distilled in vacuum to give 7.5 g of a colourless liquid, yield 91%, b.p. 98–99 °C/28 Torr. (Found: C 81.2; H 6.84; F 11.9%. Calc. for  $\text{C}_{11}\text{H}_{15}\text{F}$ : C 81.48; H 6.84; F 11.72%).  $^1\text{H NMR}$  ( $\text{CDCl}_3$ ):  $\delta$  0.93 [9H, s,  $\text{C}(\text{CH}_3)_3$ ], 5.06 [1H, d, CHF,  $J(\text{HF}) = 46$  Hz], 7.30 (5H, s, arom. H). IR ( $\nu_{\text{max}}$ ,  $\text{CCl}_4$ ):  $1455\text{ cm}^{-1}$  ( $\text{C}=\text{C}$  str.),  $1040\text{ cm}^{-1}$  ( $\text{C}-\text{H}$  def.). MS [ $m/e$  (%): 166 (4, M), 147 (4, [M-F]).

**1-Bromo-2,2-dimethylpropylbenzene (4).** Dry hydrogen bromide (5.9 g, 73.2 mmol) was absorbed in a three-necked flask containing 1-hydroxy-2,2-dimethylpropylbenzene (4.0 g, 24.4 mmol) according to the method of Norris.<sup>36a</sup> After 12 h, the reaction mixture was worked up.<sup>36a</sup> The product was distilled in vacuum to give 2.8 g of a colourless liquid, yield 50%, b.p. 96–98 °C/6 Torr,  $n_D^{21} = 1.5389$  (lit.<sup>36a-e</sup> b.p. 109 °C/10 Torr,  $n_D^{20} = 1.5398$ ; b.p. 114–115 °C/15 Torr; b.p. 103–104 °C/7.5 Torr).  $^1\text{H NMR}$  ( $\text{CDCl}_3$ ):  $\delta$  1.05 [9H, s,  $\text{C}(\text{CH}_3)_3$ ], 4.82 (1H, s, CH), 7.33 (5H, m, arom. H).

**1-Iodo-2,2-dimethylpropylbenzene (5).** Dry hydrogen iodide (9.4 g, 73.4 mmol), formed by the reaction between 66% ( $\zeta = 1.94\text{ g ml}^{-1}$ ) hydroiodic acid with an excess of phosphorus pentoxide plus a catalytic amount of red phosphorus, was absorbed in a three-necked flask containing 1-hydroxy-2,2-dimethylpropylbenzene (4.0 g, 24.4 mmol), as described by Norris.<sup>36a</sup> After a reaction time of 12 h, followed by work-up, the product was distilled in vacuum to give 4.0 g of a colourless liquid, yield 60%, b.p. 104–105 °C/8 Torr. (Found: C 48.4; H 5.62; I 45.9%. Calc. for  $\text{C}_{11}\text{H}_{15}\text{I}$ : C 48.35; H 5.50; I 46.15%).  $^1\text{H NMR}$  ( $\text{CDCl}_3$ ):  $\delta$  1.06 [9H, s,  $\text{C}(\text{CH}_3)_3$ ], 5.03 (1H, s, CH), 7.33 (5H, m, arom. H). IR ( $\nu_{\text{max}}$ ,  $\text{CCl}_4$ ):  $3035\text{ cm}^{-1}$  ( $=\text{C}-\text{H}$  str.),  $1180\text{ cm}^{-1}$  ( $\text{C}-\text{H}$  def.). MS [ $m/e$  (%): 259 (2, [M-CH<sub>3</sub>]), 147 (3, [M-I]).

**1-Methoxy-2,2-dimethylpropylbenzene (6).** This compound was prepared from 1-hydroxy-2,2-dimethylpropylbenzene (4.0 g, 24.4 mmol), dimethyl sulphate (4.4 g; 34.9 mmol) and sodium hydroxide (5.2 ml, 50%) by the phase-transfer catalysis method described by Merz.<sup>30</sup> Tetra-*n*-butylammonium hydrogen sulphate (0.05 g) was the transfer catalyst. The reaction time was 3 h, and was not optimized. After work-up, the reaction product was chromatographed on a column of alumina with cyclohexane as eluent. After collection, the eluent was evaporated and the residue distilled in vacuum to give 2.0 g of a colourless liquid, yield 45%, b.p. 77–78 °C/8 Torr (lit.<sup>37</sup> b.p. 94–95 °C/20 Torr). (Found: C 80.4; H 10.2%. Calc. for  $\text{C}_{12}\text{H}_{18}\text{O}$ : C 80.8; H 10.1%).  $^1\text{H NMR}$  ( $\text{CDCl}_3$ ):  $\delta$

0.86 [9H, s,  $\text{C}(\text{CH}_3)_3$ ], 3.20 (3H, s,  $\text{OCH}_3$ ), 7.33 (5H, s, arom. H).

**1-Acetoxy-2,2-dimethylpropylbenzene (7).** This compound was synthesized from 1-hydroxy-2,2-dimethylpropylbenzene (1.0 g, 6.1 mmol), acetic anhydride (3.8 g, 37.0 mmol) and dry pyridine (5 ml) according to the general method described by Hauser *et al.*<sup>38</sup> After work-up, the residue was distilled in vacuum to give 0.91 g of a colourless liquid, yield 73%, b.p. 103–104 °C/6 Torr (lit.<sup>37</sup> b.p. 123–124 °C/16 Torr). (Found: C 75.3; H 8.60%. Calc. for  $\text{C}_{13}\text{H}_{18}\text{O}_2$ : C 75.70; H 8.73%).  $^1\text{H NMR}$  ( $\text{CDCl}_3$ ):  $\delta$  0.97 [9H, s,  $\text{C}(\text{CH}_3)_3$ ], 2.14 (3H, s,  $\text{COCH}_3$ ), 5.60 (1H, s, CH), 7.40 (5H, s, arom. H).

**1-Trimethylsilyloxy-2,2-dimethylpropylbenzene (8).** This compound was synthesized from 1-hydroxy-2,2-dimethylpropylbenzene (0.5 g, 3.1 mmol), trimethylchlorosilane (0.5 g, 4.6 mmol) and dry pyridine (10 ml) according to the general method described by Birkhofer *et al.*<sup>39</sup> After work-up the reaction product was distilled in vacuum to give 0.65 g of a colourless liquid, yield 92%, b.p. 88–89 °C/6 Torr. (Found: C 70.9; H 9.84; Si 12.3%. Calc. for  $\text{C}_{14}\text{H}_{24}\text{OSi}$ : C 71.10; H 10.17; Si 11.90%).  $^1\text{H NMR}$  ( $\text{CDCl}_3$ ):  $\delta$  0 [9H, s,  $\text{Si}(\text{CH}_3)_3$ ], 0.95 [9H, s,  $\text{C}(\text{CH}_3)_3$ ], 4.30 (1H, s, CH), 7.33 (5H, s, arom. H). IR ( $\nu_{\text{max}}$ ,  $\text{CCl}_4$ ):  $3014\text{ cm}^{-1}$  ( $=\text{C}-\text{H}$  str.),  $1100\text{ cm}^{-1}$  ( $\text{C}-\text{O}-\text{Si}$  str.). MS [ $m/e$  (%): 236 (1, M), 179 (100, [M-t-Bu]).

**Phenyl tert-butyl ketone (pivalophenone) (17).** The methods published by Hampton *et al.*<sup>31a</sup> and Neidrig *et al.*<sup>31b</sup> were followed to give the compound, b.p. 120–121 °C/23 Torr,  $n_D^{21} = 1.5077$  (lit.<sup>31a,b</sup> b.p. 110–111 °C/18 Torr; b.p. 103–104 °C/13 Torr,  $n_D^{19,2} = 1.5086$ ).

**2-Phenyl-3,3-dimethylbutan-2-ol (12).** This compound was prepared from phenyl tert-butyl ketone (16.4 g, 0.10 mol) and methylmagnesium iodide (0.21 mol) according to Ramart-Lucas,<sup>40</sup> b.p. 120–121 °C/19 Torr,  $n_D^{22} = 1.5127$  (lit.<sup>40</sup> b.p. 116–117 °C/15 Torr,  $n_D^{25} = 1.5135$ ).

**3-Phenyl-2,2-dimethylpentan-3-ol (13).** Ethyllithium (0.23 mol) in dry diethyl ether (prepared according to Ref. 41) was added dropwise to phenyl tert-butyl ketone (17.2 g, 0.11 mol) in a three-necked flask. The reaction mixture was refluxed for 12 h, then hydrolysed with 50 ml of a saturated solution of ammonium chloride and extracted with  $3 \times 15$  ml of diethyl ether. The organic phases were collected, dried ( $\text{MgSO}_4$ ) and the ether was evaporated. The residue was distilled in vacuum to give 15.4 g of a colourless liquid, yield 75%, b.p. 97–98 °C/4 Torr,  $b_D^{25} = 1.509$  (lit.<sup>42a,b</sup> b.p. 115–116 °C/11 Torr,  $n_D^{25} = 1.5064$ ; b.p. 118–120 °C/15 Torr,  $n_D^{25} = 1.5105$ ).

**3-Phenyl-2,2-dimethylheptan-3-ol (14).** This compound was prepared from phenyl tert-butyl ketone (3.0 g, 18.5 mmol) and *n*-butyllithium (12.4 ml, 1.49 M) in hexane according to the procedure described above for 3-phenyl-2,2-dimethylpentan-3-ol. The reaction time was 24 h. After work-up 3.4 g of a colourless liquid were obtained, yield 83%, b.p. 108–109 °C/4 Torr. (Found: C 81.8; H 10.81%. Calc. for  $\text{C}_{15}\text{H}_{24}\text{O}$ : C 81.81; H 10.90%).  $^1\text{H NMR}$  ( $\text{CDCl}_3$ ):  $\delta$  0.90 [9H, s,  $\text{C}(\text{CH}_3)_3$ ], 0.85–1.40 (7H, m,  $\text{CH}_2$  and  $\text{CH}_3$ ), 1.80 (1H, s, OH), 1.70–2.10 (2H, s,  $\text{CH}_2$ ),

7.14–7.66 (5H, s, arom. H). IR ( $\nu_{\max}$ ,  $\text{CCl}_4$ ):  $3610\text{ cm}^{-1}$  (O–H str.). MS [ $m/e$  (%): 202 (14, [ $M - \text{H}_2\text{O}$ ]), 183 (100, [ $M - \text{H}_2\text{O} - \text{Et}$ ]), 163 (17, [ $M - t\text{-Bu}$ ]).

**2,2,4-Trimethylpentan-3-one (isopropyl tert-butyl ketone 18)**. This ketone was prepared by oxidation of 3-hydroxy-2,2,4-trimethylpentane (prepared by reaction between isobutyraldehyde and tert-butylmagnesium chloride) as described by Favorski and Fritzman,<sup>32a,b</sup> b.p. 134–135°C (lit.<sup>32b</sup> b.p. 134–135°C).

**3-Phenyl-2,4,4-trimethylpentan-3-ol (15)**. Isopropyl tert-butyl ketone (5.0 g, 39.1 mmol) was added dropwise to a solution of phenyllithium<sup>41</sup> (19.6 ml, 2 M) in benzene–diethyl ether (7:3) under a nitrogen atmosphere. The reaction mixture was stirred for 12 h at room temperature, then hydrolysed with 50 ml of water and worked up as described for 3-phenyl-2,2-dimethylpentan-3-ol. After distillation 4.0 g of a colourless liquid were obtained, yield 49%, b.p. 93–94°C/1–2 Torr. (Found: C 81.2; H 10.60%. Calc. for  $\text{C}_{14}\text{H}_{22}$ : C 81.55; H 10.68%).  $^1\text{H}$  NMR ( $\text{CDCl}_3$ ):  $\delta$  0.71 (3H, d,  $\text{CH}_3$ ,  $J = 7$  Hz), 0.96 [9H, s,  $\text{C}(\text{CH}_3)_3$ ], 1.10 (3H, d,  $\text{CH}_3$ ,  $J = 7$  Hz), 1.68 (1H, s, OH), 2.58 (1H, m, CH,  $J = 7$  Hz), 7.10–7.80 (5H, m, arom. H). IR ( $\nu_{\max}$ ,  $\text{CCl}_4$ ):  $3620\text{ cm}^{-1}$  (O–H str.). MS [ $m/e$  (%): 206 (1, M), 163 (18, [ $M - i\text{-Pr}$ ]), 149 (100, [ $M - t\text{-Bu}$ ]).

**2,2,4,4-Tetramethylpentan-3-one (di-tert-butyl ketone 19)**. This ketone was prepared from pivaloyl chloride and tert-butylmagnesium chloride as described in Refs 33 and 34, b.p. 152–153°C,  $n_D^{22} = 1.4187$  (lit.<sup>33,34</sup> b.p. 152–153°C; b.p. 69.5°C/48 Torr;  $n_D^{20} = 1.4192$ ;  $n_D^{25} = 1.4170$ ).

**3-Phenyl-2,2,4,4-tetramethylpentan-3-ol (16)**. This compound was synthesized from di-tert-butyl ketone and phenyllithium (prepared according to Ref. 41) by the procedure of Bartlett *et al.*,<sup>43</sup> b.p. 140–142°C/11 Torr,  $n_D^{25} = 1.5232$  (lit.<sup>4b,43</sup> b.p. 140–143°C/12 Torr; b.p. 148–151°C/15 Torr,  $n_D^{25} = 1.5230$ ).

**2-Phenyl-3,3-dimethylbutane ( $\alpha$ -t-butylstyrene, 20)**. Triphenylmethylphosphorane was synthesized from triphenylmethylphosphonium bromide (16.0 g, 44.7 mmol) and *n*-butyllithium (30 ml, 0.49 M), as described in Ref. 44. Phenyl tert-butyl ketone (6.0 g, 44.7 mmol) dissolved in 50 ml of dry diethyl ether was added and the reaction mixture was refluxed for 20 h. The mixture was then hydrolysed with 50 ml of water, the phases were separated and the aqueous phase was extracted with two 40-ml portions of diethyl ether. The organic phases were collected, dried ( $\text{MgSO}_4$ ) and the solvent was evaporated, leaving a liquid residue, which was chromatographed on a column of alumina with hexane as eluent. Two fractions were collected (with  $R_f$  values of 0.72 and 0.33). The solvent was evaporated from the first fraction, leaving 4.4 g of a colourless liquid, yield 73%, b.p. 91–92°C/15 Torr,

$n_D^{22} = 1.5013$  (lit.<sup>45a,b</sup> b.p. 88–92°C/15 Torr).  $^1\text{H}$  NMR ( $\text{CDCl}_3$ ):  $\delta$  1.11 [9H, s,  $\text{C}(\text{CH}_3)_3$ ], 4.81 (1H, d,  $\text{CH}_2$ ,  $J = 1$  Hz), 5.20 (1H, d,  $\text{CH}_2$ ,  $J = 1$  Hz), 7.25 (5H, s, arom. H). Evaporation of the solvent from the second fraction and NMR analysis showed the residue to be unreacted starting material.

**Mixture of Z- and E-3-phenyl-4,4-dimethylpent-2-ene (21+22)**. Triphenylethylidenephosphorane was synthesized from triphenylethylphosphonium bromide (5.53 g, 14.9 mmol) and *n*-butyllithium (10 ml, 1.49 M) in hexane. Phenyl tert-butyl ketone (2.0 g, 14.9 mmol) dissolved in 25 ml of dry diethyl ether was added and the procedure described above for 2-phenyl-3,3-dimethylbutene was followed. After work-up 2.2 g of a colourless liquid were obtained, yield 85%, b.p. 92–93°C/12 Torr,  $n_D^{22} = 1.5140$  (lit.<sup>45c</sup> b.p. 91–93°C/12 Torr).  $^1\text{H}$  NMR ( $\text{CDCl}_3$ ):  $\delta$  1.33 [m,  $\text{C}(\text{CH}_3)_3$ ], 1.85 (d,  $\text{CH}_3$ ,  $J = 8$  Hz), 5.24 (q, CH,  $J = 8$  Hz), 6.80–7.40 (m, arom. H + CH,  $J = 8$  Hz partly overlapping). A mixture of two isomers with the methyl group *cis* and *trans* to the phenyl group was obtained.

**3-Phenyl-2,2-dimethylbutane (9)**. 2-Phenyl-3,3-dimethylbutene (2.5 g, 15.6 mmol) was dissolved in 75 ml of absolute ethanol. Palladium (10% on charcoal, 0.4 g) was added and the mixture was hydrogenated in a Parr apparatus at a hydrogen pressure of 490 kPa. When the theoretical amount of hydrogen had been absorbed, the reaction mixture was filtered, the ethanol evaporated and the residue chromatographed on a column of alumina with hexane as eluent. Evaporation of the solvent left 1.7 g of a clear liquid, yield 70%, b.p. 77–78°C/8 Torr,  $n_D^{21} = 1.4951$  (lit.<sup>46</sup> b.p. 205–207°C,  $n_D^{25} = 1.4942$ ).  $^1\text{H}$  NMR ( $\text{CDCl}_3$ ):  $\delta$  0.86 [9H, s,  $\text{C}(\text{CH}_3)_3$ ], 1.24 (3H, d,  $\text{CH}_3$ ,  $J = 7$  Hz), 2.57 (1H, q, CH,  $J = 7$  Hz), 7.21 (5H, s, arom. H).

**3-Phenyl-2,2-dimethylpentane (10)**. A mixture of Z- and E-3-phenyl-4,4-dimethylpent-2-ene (1.0 g, 5.8 mmol) was hydrogenated and worked up as described for 3-phenyl-2,2-dimethylbutane. After work-up 0.64 g of a colourless liquid remained, yield 64%, b.p. 93–94°C/8 Torr,  $n_D^{21} = 1.4921$  (lit.<sup>46</sup> b.p. 221–223°C,  $n_D^{25} = 1.4912$ ).  $^1\text{H}$  NMR ( $\text{CDCl}_3$ ):  $\delta$  0.66 (3H, t,  $\text{CH}_3$ ,  $J = 7$  Hz), 0.87 [9H, s,  $\text{C}(\text{CH}_3)_3$ ], 1.33–2.40 [3H, m, CH and  $\text{CH}_2$ ,  $J(\text{CH}_2) = 7$  Hz], 7.19 (5H, s, arom. H).

## Acknowledgements

We express our thanks to Dr Robert E. Carter for stimulating discussions, comments on the manuscript and linguistic criticism. We are also grateful to Professor Börje Wickberg for his synthetic support, Dr Tommy Liljefors for placing his versions of the Allinger MM1/MMP1 and MM2/MMP2 programs at our disposal and Ms Evabritt Sandmark for typing the manuscript.

## REFERENCES

1. For studies of ring-substituted TNB compounds see (a) R. E. Carter, J. Marton and K. I. Dahlqvist, *Acta Chem. Scand.*

**24**, 195 (1970); (b) B. Nilsson, R. E. Carter, K. I. Dahlqvist and J. Marton, *Org. Magn. Reson.* **4**, 95 (1972); (c) B.

- Nilsson, *Mol. Phys.* **27**, 625 (1974); (d) B. Nilsson, P. Martinson, K. Olsson and R. E. Carter, *J. Am. Chem. Soc.* **96**, 3190 (1974); (e) B. Nilsson, P. Martinson, K. Olsson and R. E. Carter, *J. Am. Chem. Soc.* **95**, 5615 (1973); (f) R. E. Carter, B. Nilsson and K. Olsson, *J. Am. Chem. Soc.* **97**, 6155 (1975); (g) R. E. Carter and P. Stilbs, *J. Am. Chem. Soc.* **98**, 7515 (1976); (h) S. Andersson, R. E. Carter and T. Drakenberg, *Acta Chem. Scand. Ser. B* **34**, 661 (1980).
2. J. M. A. Baas and A. Sinnema, *Recl. Trav. Chim. Pays-Bas* **92**, 899 (1973).
  3. (a) J. M. Reuvers, A. Sinnema, Th. J. Nieuwstad, F. van Rantwijk and H. van Bekkum, *Tetrahedron* **27**, 3713 (1971); (b) J. M. Reuvers, H. van Bekkum and B. M. Wepster, *Tetrahedron* **26**, 2683 (1970).
  4. (a) J. M. A. Baas, *Recl. Trav. Chim. Pays-Bas* **91**, 1287 (1972); (b) J. M. A. Baas, J. M. van der Toorn and B. M. Wepster, *Recl. Trav. Chim. Pays-Bas* **93**, 133 (1974).
  5. (a) R. E. Gall, D. Landman, G. P. Newsoroff and S. Sternhell, *Austr. J. Chem.* **25**, 109 (1972); (b) G. P. Newsoroff and S. Sternhell, *Tetrahedron Lett.* 2539 (1967).
  6. (a) J. Peeling, J. B. Rowbotham, L. Ernst and T. Schaefer, *Can. J. Chem.* **52**, 2414 (1974); (b) U. Berg and U. Sjöstrand, *Org. Magn. Reson.* **11**, 555 (1978).
  7. (a) S. Glasstone, K. J. Laidler and H. Eyring, in *The Theory of Rate Processes*, p. 195. McGraw-Hill, New York (1941); (b) G. Binsch, in *Dynamic Nuclear Magnetic Resonance Spectroscopy*, edited by L. M. Jackman and F. A. Cotton, pp. 45-76. Interscience, New York, (1975).
  8. B. Fuhr, B. W. Goodwin, H. M. Hutton and T. Schaefer, *Can. J. Chem.* **48**, 1558 (1970).
  9. (a) N. L. Allinger, M. T. Tribble, M. A. Miller and D. H. Wertz, *J. Am. Chem. Soc.* **93**, 1637 (1971); (b) D. H. Wertz and N. L. Allinger, *Tetrahedron* **30**, 1597 (1974); (c) N. L. Allinger, J. T. Sprague and T. Liljefors, *J. Am. Chem. Soc.* **98**, 5100 (1974); (d) N. L. Allinger and J. T. Sprague, *J. Am. Chem. Soc.* **95**, 3893 (1973); (e) T. Liljefors and N. L. Allinger, *J. Am. Chem. Soc.* **98**, 2745 (1976); (f) R. E. Carter and T. Liljefors, *Tetrahedron* **32**, 2915 (1976); (g) A. Meyer and N. L. Allinger, *Tetrahedron* **31**, 1971 (1975).
  10. MM1/MMP1 program [QCPE, No. 318], kindly placed at our disposal by Dr T. Liljefors, University of Lund.
  11. N. L. Allinger, *J. Am. Chem. Soc.* **99**, 8127 (1977).
  12. MMP2 program, kindly placed at our disposal by Dr T. Liljefors, University of Lund.
  13. (a) G. C. Levy and G. L. Nelson, *Carbon-13 Nuclear Magnetic Resonance for Organic Chemists*, Wiley, New York (1972); (b) F. Wehrli and T. Wirthlin, *Interpretation of Carbon-13 NMR Spectra*, London Corp. (1976); (c) E. Breitmaier and W. Voelter, *<sup>13</sup>C NMR Spectroscopy*, Verlag Chemie, Berlin (1974).
  14. J. A. Pople, W. G. Schneider and H. J. Bernstein, *High Resolution Nuclear Magnetic Resonance*, Chapt. 8-10. McGraw-Hill, New York (1959).
  15. (a) T. Schaefer, C. M. Wong and K. C. Tam, *Can. J. Chem.* **47**, 3688 (1969); (b) J. Peeling, T. Schaefer and C. M. Wong, *Can. J. Chem.* **48**, 2839 (1970); (c) J. B. Rowbotham, A. F. Janzen, J. Peeling and T. Schaefer, *Can. J. Chem.* **52**, 481 (1974); (d) H. G. Gyulai, B. J. Fuhr, H. M. Hutton and T. Schaefer, *Can. J. Chem.* **48**, 3877 (1970); (e) J. Peeling, L. Ernst and T. Schaefer, *Can. J. Chem.* **52**, 849 (1974); (f) K. Chum, J. B. Rowbotham and T. Schaefer, *Can. J. Chem.* **52**, 3489 (1974); (g) W. J. Parr and T. Schaefer, *Acc. Chem. Res.* **13**, 400 (1980); (h) T. Schaefer, L. J. Kruczynski and W. J. Parr, *Can. J. Chem.* **54**, 3210 (1976); (i) T. Schaefer, W. Danchura and W. Niemezura, *Can. J. Chem.* **56**, 36 (1978); (k) T. Schaefer, W. Niemezura, R. Sebastian, L. J. Kruczynski and W. Danchura, *Can. J. Chem.* **58**, 1178 (1980); (l) T. Schaefer, W. Danchura, W. Niemezura and J. Peeling, *Can. J. Chem.* **56**, 2442 (1978).
  16. C. A. Cupas, J. M. Bollinger and M. Haslanger, *J. Am. Chem. Soc.* **90**, 5502 (1968).
  17. (a) A. Mannschreck and L. Ernst, *Chem. Ber.* **104**, 228 (1971); (b) A. Mannschreck and L. Ernst, *Tetrahedron Lett* 5939 (1968).
  18. J. Elzinga and H. Hogeveen, *J. Org. Chem.* **46**, 1358 (1981)
  19. For further details, see S. Andersson, Thesis, University of Lund (1982) (available from the author on request).
  20. J. E. Anderson, H. Pearson and D. I. Rawson, *J. Chem. Soc., Chem. Commun.* 95 (1973).
  21. (a) A. Gordon and R. Ford, *The Chemist's Companion, A Handbook of Practical Data, Techniques and References*. Wiley, New York (1972); (b) B. Shklover, P. Adjasuren, I. Cynkier, B. Jablskov, A. Ganiushkin and Y. Struchkov, *Zh. Struct. Khim.* **21**, 112 (1980).
  22. D. Höfner, S. Lesko and G. Binsch, *Org. Magn. Reson.* **11**, 179 (1978), and references cited therein.
  23. B. L. Hawkins, W. Bremser, S. Borcic and J. D. Roberts, *J. Am. Chem. Soc.* **93**, 4472 (1971).
  24. (a) J. E. Anderson and H. Pearson, *Tetrahedron Lett.* 2779 (1972); (b) J. E. Anderson and H. Pearson, *J. Chem. Soc., Chem. Commun.* 871 (1971); (c) J. E. Anderson and H. Pearson, *J. Am. Chem. Soc.* **97**, 764 (1975); (d) J. E. Anderson and H. Pearson, *J. Chem. Soc. B* 1209 (1971); (e) J. E. Anderson and H. Pearson, *J. Chem. Soc. Chem. Commun.* 908 (1972).
  25. W. Freitag and H. J. Schneider, *Isr. J. Chem.* **20**, 153 (1980).
  26. C. H. Bushweller and W. G. Anderson, *Tetrahedron Lett.* 1811 (1972).
  27. D. Hounshell, L. Iroff, D. Iversen, R. Wroczynski and K. Mislow, *Isr. J. Chem.* **20**, 65 (1980).
  28. A. Bygdén, *Chem. Ber.* **45**, 3479 (1912).
  29. J. B. Conant and A. H. Blatt, *J. Am. Chem. Soc.* **50**, 554 (1928).
  30. A. Merz, *Angew. Chem.* **85**, 868 (1973).
  31. (a) J. Hampton, A. Leo and F. Westheimer, *J. Am. Chem. Soc.* **78**, 306 (1956); (b) H. Neidrig, P. Funck, R. Baker and W. Kreisser, *J. Am. Chem. Soc.* **72**, 4617 (1950).
  32. (a) R. Favorski and P. Fritzman, *J. Russ. Phys. Chem. Soc.* **44**, 1351 (1912); (b) R. Favorski and P. Fritzman, *J. Prakt. Chem.* **2**, **88**, 651 (1912).
  33. W. Percival, R. Wagner and N. Cook, *J. Am. Chem. Soc.* **75**, 3731 (1953).
  34. J. Dubois, B. Leheup, F. Hennequin and P. Bauer, *Bull. Soc. Chim. Fr.* 1150 (1967).
  35. S. Winstein and B. K. Morse, *J. Am. Chem. Soc.* **74**, 1133 (1952).
  36. (a) J. F. Norris, *J. Am. Chem. Soc.* **38**, 641 (1907); (b) A. Lepin, *J. Russ. Phys. Chem. Soc.* **44**, 1178 (1912); (c) A. Lepin, *Chem. Zentralbl.* **II** 2081 (1912); (d) P. Skell and C. R. Hauser, *J. Am. Chem. Soc.* **64**, 2633 (1942); (e) T. Tsatsas, *Justus Liebigs Ann. Chem.* vol. **12**, **I** 342, 374 (1946).
  37. A. Ford, W. Trompson and D. Marvel, *J. Am. Chem. Soc.* **57**, 2619, 2622 (1935).
  38. C. R. Hauser, B. Hudson, B. Abramovitch and H. Shivers, *Org. Synth. Coll. Vol.* **1**, 142 (1941).
  39. L. Birkhofer and A. Ritter, *Angew. Chem., Int. Ed. Engl.* **4**, 417 (1965).
  40. M. Ramart-Lucas, *C.R. Acad. Sci.* **150**, 1059 (1912).
  41. Houben-Weyl, *Methoden der Organischen Chemie*, Ed. 4, Vol. 13, p. 137. Georg Thieme Verlag, Stuttgart (1970).
  42. (a) M. Ramart-Lucas, *C.R. Acad. Sci.* **154**, 709 (1913); (b) M. Ramart-Lucas, *Ann. Chim. Phys.* vol. **8**, **30**, 356 (1913).
  43. P. D. Bartlett, R. Steadman, T. T. Tidwell and W. P. Weber, *Tetrahedron Lett.* 2915 (1970).
  44. G. Wittig, *Org. Synth. Coll. Vol.* **1**, 530 (1941).
  45. (a) M. Ramart-Lucas, *C.R. Acad. Sci.* **152**, 1772 (1913); (b) M. Ramart-Lucas, *Ann. Chim. Phys.* vol. **8**, **30**, 382 (1913); (c) M. Ramart-Lucas, *Ann. Chim. Phys.* vol. **8**, **30**, 388 (1913).
  46. R. C. Huston and I. A. Kaye, *J. Am. Chem. Soc.* **64**, 1576 (1942).

Received 30 March 1983; accepted 16 May 1983